INTERNATIONAL JOURNAL OF ROBUST AND NONLINEAR CONTROL
Int. J. Robust. Nonlinear Control (2011)
Published online in Wiley Online Library (wileyonlinelibrary.com). DOI: 10.1002/rnc.1694

Robust impulsive control of motion systems with uncertain friction

N. van de Wouw[1,*,†] and R. I. Leine[2]

[1]*Department of Mechanical Engineering, Eindhoven University of Technology, P.O. Box 513, 5600 MB Eindhoven, The Netherlands*
[2]*Department of Mechanical and Process Engineering, Institute of Mechanical Systems, ETH Zurich, CH-8092 Zürich, Switzerland*

SUMMARY

In this paper, we consider the robust set-point stabilization problem for motion systems subject to friction. Robustness aspects are particularly relevant in practice, where uncertainties in the friction model are unavoidable. We propose an impulsive feedback control design that robustly stabilizes the set-point for a class of position-, velocity- and time-dependent friction laws with uncertainty. Moreover, it is shown that this control strategy guarantees the finite-time convergence to the set-point which is a favorable characteristic of the resulting closed loop from a transient performance perspective. The results are illustrated by means of a representative motion control example. Copyright © 2011 John Wiley & Sons, Ltd.

Received 28 April 2010; Revised 18 November 2010; Accepted 8 December 2010

KEY WORDS: robust stabilisation; impulsive control; friction; motion control

1. INTRODUCTION

In this paper, we consider the robust set-point stabilization problem for motion control systems with uncertain friction using an impulsive control strategy. It is well known that controlled motion systems with friction exhibit many undesirable effects such as stick-slip limit cycling, large settling times and non-zero steady-state errors, see e.g. [1–8]. In the literature many different approaches towards the control of motion systems with friction have been proposed, such as PID control design, friction compensation, dithering-based approaches, adaptive techniques and impulsive control strategies. As shown e.g. in [3, 6], PID control techniques may suffer from an instability phenomenon known as hunting limit cycling. Many friction compensation approaches are available in the literature (see, for example, [3–10]) and have successfully been applied in practice, although it is widely recognized that the undercompensation and overcompensation of friction (due to inevitable friction modelling errors) may lead to non-zero steady-state errors and limit cycling [8, 11, 12]. Examples of adaptive compensation approaches are an adaptive friction compensation strategy reported in [13] and a model reference adaptive control scheme proposed in [14]. Dithering-based approaches, see e.g. [3, 15–17], aim at smoothing the discontinuity induced by (Coulomb) friction by the introduction of high-frequency excitations and thereby aim to avoid non-zero steady-state errors. The basic idea behind impulsive control strategies is the introduction of controlled impulsive forces when the system gets stuck at a non-zero steady-state error (due to the stiction effect of friction), see e.g. [1, 3, 18–28]. One of the key practical problems faced

*Correspondence to: N. van de Wouw, Department of Mechanical Engineering, Eindhoven University of Technology, P.O. Box 513, 5600 MB Eindhoven, The Netherlands.
†E-mail: N.v.d.wouw@tue.nl

in any of those 'friction-beating' strategies is the fact that friction is a phenomenon which is particularly hard to model accurately, especially due to e.g. changing environmental conditions such as lubrication conditions, temperature, wear, humidity etc. [3–5]. It is therefore of the utmost importance to develop stabilizing controllers that are robust against uncertainties in the friction.

Here, we propose an impulsive feedback control strategy which guarantees the robust stability of the set-point in the face of frictional uncertainties, where we consider a large class of position-dependent, velocity-dependent and time-varying friction models. The practical feasibility of impulsive force manipulation for the positioning of motion control systems has been illustrated in [19–24, 26, 27]. Moreover, different impulsive feedback control strategies have been proposed in [24, 25, 27, 28]. However, rigorous stability analyses of the closed-loop system are rare, especially when accounting for uncertainties in the friction model. A notable exception is the recent work in [28] in which an impulsive feedback law similar to the one proposed in this paper has been studied. The common idea behind this impulsive control law is that, when the system reaches the stick phase at a non-zero regulation error, an impulsive force is applied, which kicks the system out of the stick phase and whose magnitude is dependent on the positioning error. The current work differs from and extends the work in [28] in the following ways. First, in this paper we provide a proof for the robust set-point stability for a class of set-valued Coulomb friction models where the friction coefficient may be position-dependent, velocity-dependent and time-dependent, whereas in [28] only a stability analysis for uncertain, but *constant*, friction coefficients is given. Given the fact that position-dependencies, velocity-dependencies (think of e.g. the Stribeck effect) and time-dependent frictional characteristics (due to e.g. changing temperature, humidity or lubrication conditions) are always present in practice, such an extension is very relevant for applications. Second, in [28] a combination of an impulsive controller with a smooth linear position-error feedback controller is considered. In the current work, we consider an impulsive controller in combination with a more general linear state-feedback controller. As also stated in [28], such an extension is highly desirable from a performance perspective. Finally, in the current paper we provide a proof for the *finite-time* stability of the set-point, as opposed to mere asymptotic stability in [28].

Resuming, the main contributions of the current paper are as follows. First, we propose an impulsive feedback control design for a motion control system consisting of a controlled inertia subject to friction modelled by a general class of set-valued, position-dependent, velocity-dependent and time-varying friction models. Second, a stability analysis is performed to guarantee the robust stability of the set-point in the face of uncertainties in the friction. Third, we show that the stability achieved is symptotic (i.e. attractivity in finite time to the set-point is guaranteed).

The outline of the paper is as follows. In Section 2, the control problem tackled in this paper is formalized. In Section 3, the impulsive control design is introduced. The robust (finite-time) stability analysis of the impulsive closed-loop system is presented in Section 4. The effectiveness of the control design and its robustness properties are illustrated by means of an example in Section 5. Finally, concluding remarks are presented in Section 6. Some of the proofs are collected in the appendix.

2. CONTROL PROBLEM FORMULATION

Consider a one-degree-of-freedom mechanical system consisting of an inertia with mass m which is in frictional contact with a support, being a flat horizontal plane (see Figure 1). We denote

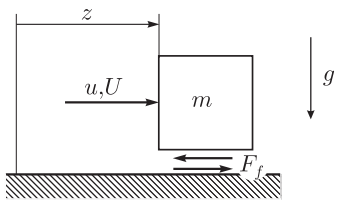

Figure 1. Mechanical motion system with control input.

DOI: 10.1002/rnc

the position of the inertia by z and its velocity by $\dot{z}$ whenever it exists. A friction force F_f acts between the mass and the support under the influence of a normal force mg, where g denotes the gravitational acceleration. The control input consists of a finite control force u and an impulsive control force U. The dynamics of the control system is described by the equation of motion (the balance of linear momentum)

$$m\ddot{z} = u + F_f(z, \dot{z}, t) \tag{1}$$

and the impact equation

$$m(\dot{z}^+(t_j) - \dot{z}^-(t_j)) = U, \tag{2}$$

which relates the difference between the post-impact velocity $\dot{z}^+(t_j)$ and the pre-impact velocity $\dot{z}^-(t_j)$ to the impulsive control force U at time t_j. It is tacitly assumed that the impulsive force U is such that the velocity $\dot{z}(t)$ is of locally bounded variation. A proof for the validity of this assumption can be found in [29].

The friction force $F_f(z, \dot{z}, t)$ is assumed to obey the following set-valued force law:

$$F_f(z, \dot{z}, t) \in -mg\mu(z, \dot{z}, t)\,\mathrm{Sign}(\dot{z}), \tag{3}$$

where $\mathrm{Sign}(\cdot)$ denotes the set-valued sign function defined by

$$\mathrm{Sign}(y) := \begin{cases} \{-1\}, & y < 0 \\ [-1, 1], & y = 0 \\ \{1\}, & y > 0 \end{cases}. \tag{4}$$

Moreover, $\mu(z, \dot{z}, t)$ denotes the friction coefficient that may depend on z and $\dot{z}$, which are both functions of time, and may also depend explicitly on time t. Note that (3) represents a rather large class of friction models including possibly position-dependent friction, velocity-dependent effects, such as the Stribeck effect, and time-dependent friction (which can occur in practice due to changing temperature/humidity of the contact, wear or changing lubrication conditions). Moreover, (3) represents a set-valued friction model to account for the stiction effect induced by dry friction. Despite the fact that (3) represents a static friction model, the explicit time-dependency can also account for certain effects encountered in dynamic friction models. In the remainder of this paper, we adopt the following assumption on the friction coefficient.

Assumption 1
The friction coefficient $\mu(z, \dot{z}, t)$ is lower bounded by $\underline{\mu}$ and upper bounded by $\overline{\mu}$, i.e. it holds that

$$\underline{\mu} \leqslant \mu(z, \dot{z}, t) \leqslant \overline{\mu} \quad \forall t, z, \dot{z} \in \mathbb{R}, \tag{5}$$

for some $0 < \underline{\mu} \leqslant \overline{\mu}$.

In the remainder of this paper, we express the dynamics of the system in first-order form by using the state vector $\boldsymbol{x} = [x_1 \;\; x_2]^{\mathrm{T}} := [z \;\; \dot{z}]^{\mathrm{T}}$. The impulsive and non-impulsive dynamics of the system can be represented by a (in general non-autonomous) first-order measure differential inclusion [30–32]:

$$\begin{aligned} \mathrm{d}x_1 &= x_2\,\mathrm{d}t \\ \mathrm{d}x_2 &\in -g\mu(x_1, x_2, t)\mathrm{Sign}(x_2)\,\mathrm{d}t + \frac{1}{m}\,\mathrm{d}p, \end{aligned} \tag{6}$$

where

$$\mathrm{d}p = u\,\mathrm{d}t + U\,\mathrm{d}\eta \tag{7}$$

is the differential measure of the control input, $\mathrm{d}t$ is the Lebesgue measure and $\mathrm{d}\eta$ is a differential atomic measure consisting of a sum of Dirac point measures [32, 33]. The decomposition of the

DOI: 10.1002/rnc

control force as in (7) implies that the differential measure $\mathrm{d}\boldsymbol{x}$ of the state can be decomposed as follows: $\mathrm{d}\boldsymbol{x}=\dot{\boldsymbol{x}}\,\mathrm{d}t+(\boldsymbol{x}^+-\boldsymbol{x}^-)\mathrm{d}\eta$. Such a decomposition implies that $\boldsymbol{x}(t)$ is a special function of locally bounded variation [31]. The state $\boldsymbol{x}(t)$ admits at each time-instant t a left and right limit $\boldsymbol{x}^-(t_j)=\lim_{t\uparrow t_j}\boldsymbol{x}(t)$, $\boldsymbol{x}^+(t_j)=\lim_{t\downarrow t_j}\boldsymbol{x}(t)$, as $\boldsymbol{x}(t)$ is of (special) locally bounded variation. The time-evolution of $\boldsymbol{x}(t)$ is governed by the integration process $\boldsymbol{x}^+(t_1)=\boldsymbol{x}^-(t_0)+\int_{[t_0,t_1]}\mathrm{d}\boldsymbol{x}$, where $[t_0,t_1]$ denotes the compact time-interval between t_0 and $t_1\geqslant t_0$.

Now let us state the control problem considered in this paper.

Problem 1
Design a control law for u and U for system (6), (7) such that $\boldsymbol{x}=\boldsymbol{0}$ is a robustly globally uniformly attractively stable equilibrium point of the closed-loop system for a class of uncertain friction models of the form (3) satisfying Assumption 1.

The attraction in Problem 1 can be asymptotic or symptotic, with which we mean attraction to the equilibrium in infinite or finite time, respectively. The controller proposed in this paper will induce stability and finite-time attractivity, i.e. symptotic stability.[‡]

3. IMPULSIVE FEEDBACK CONTROL DESIGN

In order to solve Problem 1, we adopt a proportional-derivative (state-)feedback control law for u in (7) of the form

$$u(x_1,x_2)=-k_1x_1-k_2x_2,\quad k_1,k_2>0, \tag{8}$$

together with an impulsive feedback control law for U in (7) of the form

$$U(x_1,x_2^-)=\begin{cases}k_3(x_1) & \text{if } (x_2^-=0)\wedge\left(|x_1|\leqslant\dfrac{mg\overline{\mu}}{k_1}\right)\\ 0 & \text{else}\end{cases}, \tag{9}$$

where the constants k_1, k_2 and the function $k_3(x_1)$ are to be designed. The resulting closed-loop dynamics can be formulated in terms of a measure differential inclusion:

$$\begin{aligned}&\mathrm{d}x_1=x_2\,\mathrm{d}t\\ &\mathrm{d}x_2\in\left(-\frac{k_1}{m}x_1-\frac{k_2}{m}x_2-g\mu(x_1,x_2,t)\mathrm{Sign}(x_2)\right)\mathrm{d}t+\frac{1}{m}U(x_1,x_2^-)\,\mathrm{d}\eta.\end{aligned} \tag{10}$$

In between impulsive control actions, the non-impulsive dynamics is described by the differential inclusion

$$\begin{aligned}&\dot{x}_1=x_2\\ &\dot{x}_2\in-\frac{k_1}{m}x_1-\frac{k_2}{m}x_2-g\mu(x_1,x_2,t)\mathrm{Sign}(x_2).\end{aligned} \tag{11}$$

The state of the system may jump at impulsive time-instants t_j for which $U\neq 0$, i.e. for time instants at which

$$x_2^-(t_j)=0,\quad |x_1(t_j)|\leqslant\frac{mg\overline{\mu}}{k_1}, \tag{12}$$

[‡]For a definition of symptotic stability we refer to e.g. [32].

DOI: 10.1002/rnc

according to the state reset map

$$\begin{aligned} x_1^+(t_j) &= x_1^-(t_j) \\ x_2^+(t_j) &= x_2^-(t_j) + \frac{k_3(x_1^-(t_j))}{m}. \end{aligned} \tag{13}$$

In the remainder we will denote $x_1(t_j)=x_1^-(t_j)=x_1^+(t_j)$ since the position $x_1(t)=z(t)$ is an absolutely continuous function of time.

3.1. Analysis of the non-impulsive closed-loop dynamics

In this section, we study properties of the solutions of the non-impulsive closed-loop dynamics described by the differential inclusion (11) that are important for the stability analysis pursued in Section 4.

If $x_2(t)\neq 0$, then the differential inclusion (11) reduces to the nonlinear differential equation

$$\begin{aligned} \dot{x}_1 &= x_2 \\ \dot{x}_2 &= -\frac{k_1}{m}x_1 - \frac{k_2}{m}x_2 \pm g\mu(x_1, x_2, t). \end{aligned} \tag{14}$$

In the following we will regard the nonlinear term $g\mu(x_1, x_2, t)$ to be a time-varying input $g\mu(t)$ with $\mu(t):=\mu(x_1(t), x_2(t), t)$, which obeys Assumption 1, i.e. $\underline{\mu}\leqslant\mu(t)\leqslant\bar{\mu}, \forall t$. Hence, the closed-loop non-impulsive dynamics for $x_2(t)\neq 0$ is described by the linear differential equation

$$\begin{aligned} \dot{x}_1 &= x_2 \\ \dot{x}_2 &= -\omega_n^2 x_1 - 2\zeta\omega_n x_2 + f(t) \end{aligned} \tag{15}$$

with time-varying input $f(t):=-g\mu(t)\text{Sign}(x_2(t))$, undamped eigenfrequency $\omega_n=\sqrt{k_1/m}$ and damping ratio $\zeta=(k_2/(2\sqrt{k_1 m}))>0$ and $g\underline{\mu}\leqslant f(t)\leqslant g\overline{\mu}\ \forall t$. Consider the case that the controller parameters k_1 and k_2 are designed such that $\zeta>1$. Denote

$$\lambda_1 := -\omega_n\zeta + \omega_n\sqrt{\zeta^2-1}, \quad \lambda_2 := -\omega_n\zeta - \omega_n\sqrt{\zeta^2-1}, \tag{16}$$

and note that $\lambda_1\lambda_2=\omega_n^2$, $\lambda_1+\lambda_2=-2\zeta\omega_n$ and $\lambda_2<\lambda_1<0$. We denote the arbitrary initial condition as

$$x_1(t_0)=x_{10}, \quad x_2(t_0)=x_{20}. \tag{17}$$

Let $(x_1(t), x_2(t))$ denote the solution of the initial value problem (15), (17) on a time interval for which $x_2(t)$ does not change sign. Furthermore, let $(\underline{x}_1(t), \underline{x}_2(t))$ denote the solution of the initial value problem (15), (17) for $\mu(t)=\underline{\mu}, \forall t$, and $(\overline{x}_1(t), \overline{x}_2(t))$ for $\mu(t)=\overline{\mu}, \forall t$. The following proposition explicates that $\underline{x}_i(t)$ and $\overline{x}_i(t)$ characterize bounds on $x_i(t)$ $(i=1,2)$. Herein, we use the following definitions:

$$\underline{c} := \frac{mg\underline{\mu}}{k_1} = \frac{g\underline{\mu}}{\lambda_1\lambda_2}, \quad \overline{c} := \frac{mg\overline{\mu}}{k_1} = \frac{g\overline{\mu}}{\lambda_1\lambda_2}. \tag{18}$$

Proposition 1

The solutions $(\underline{x}_1(t), \underline{x}_2(t))$ and $(\overline{x}_1(t), \overline{x}_2(t))$ satisfy

$$\begin{aligned} \underline{x}_1(t) &= s_1(t-t_0)x_{10} + s_2(t-t_0)x_{20} - \underline{c}(1-s_1(t-t_0)), \\ \underline{x}_2(t) &= \dot{s}_1(t-t_0)x_{10} + \dot{s}_2(t-t_0)x_{20} - \lambda_1\lambda_2\underline{c}s_2(t-t_0) \end{aligned} \tag{19}$$

and

$$\begin{aligned} \overline{x}_1(t) &= s_1(t-t_0)x_{10} + s_2(t-t_0)x_{20} - \overline{c}(1-s_1(t-t_0)), \\ \overline{x}_2(t) &= \dot{s}_1(t-t_0)x_{10} + \dot{s}_2(t-t_0)x_{20} - \lambda_1\lambda_2\overline{c}s_2(t-t_0) \end{aligned} \tag{20}$$

DOI: 10.1002/rnc

with the definitions for $\underline{c}$ and $\overline{c}$ as in (18) and $s_1(t)$, $s_2(t)$ defined by

$$s_1(t)=\frac{\lambda_2}{\lambda_2-\lambda_1}e^{\lambda_1 t}-\frac{\lambda_1}{\lambda_2-\lambda_1}e^{\lambda_2 t} \quad \text{and} \quad s_2(t)=\frac{1}{\lambda_2-\lambda_1}(-e^{\lambda_1 t}+e^{\lambda_2 t}). \tag{21}$$

Moreover, the solution $(x_1(t), x_2(t))$ is lower and upper bounded by the solutions $(\underline{x}_1(t), \underline{x}_2(t))$ and $(\overline{x}_1(t), \overline{x}_2(t))$ according to

$$\begin{aligned} &x_2>0: \quad \overline{x}_1(t)\leqslant x_1(t)\leqslant \underline{x}_1(t), \quad \overline{x}_2(t)\leqslant x_2(t)\leqslant \underline{x}_2(t) \quad \text{for } 0\leqslant t-t_0\leqslant \frac{1}{\lambda_2-\lambda_1}\ln\frac{\lambda_1}{\lambda_2},\\ &x_2<0: \quad \overline{x}_1(t)\geqslant x_1(t)\geqslant \underline{x}_1(t), \quad \overline{x}_2(t)\geqslant x_2(t)\geqslant \underline{x}_2(t) \quad \text{for } 0\leqslant t-t_0\leqslant \frac{1}{\lambda_2-\lambda_1}\ln\frac{\lambda_1}{\lambda_2}. \end{aligned} \tag{22}$$

Proof
The proof is given in Appendix A. □

3.2. Impulsive controller design

Let us first explain the rationale behind the design of the controller (7)–(9). Hereto, consider the case that $\mu(x_1, x_2, t)=\mu$, with μ a constant, and consider the system without the impulsive part of the controller (i.e. $k_3(x_1)=0$ in (9)). In this case the closed-loop system is a PD-controlled inertia with Coulomb friction which exhibits an equilibrium set defined by $\{\boldsymbol{x}\in\mathbb{R}^2 \,|\, |x_1|\leqslant(mg\mu/k_1)\wedge x_2=0\}$. Clearly, the closed-loop system will then ultimately converge to the equilibrium set and an undesirable non-zero steady-state error will in general result. This attraction can either occur in a finite time or the solution can approach the equilibrium set asymptotically [34, 35]. Note that for (non-constant) friction coefficients $\mu(x_1, x_2, t)$ satisfying Assumption 1, the closed-loop system without impulsive control will exhibit a time-varying stick set $\mathscr{E}(t)$ that satisfies $\underline{\mathscr{E}}\subseteq\mathscr{E}(t)\subseteq\overline{\mathscr{E}} \quad \forall t$, where $\underline{\mathscr{E}}=\{\boldsymbol{x}\in\mathbb{R}^2 \,|\, |x_1|\leqslant(mg\underline{\mu}/k_1)\wedge x_2=0\}$, $\overline{\mathscr{E}}=\{\boldsymbol{x}\in\mathbb{R}^2 \,|\, |x_1|\leqslant(mg\overline{\mu}/k_1)\wedge x_2=0\}$ are the minimal and maximal stick sets, respectively. A point $\boldsymbol{x}^*=[x_1^* \quad x_2^*]^{\mathrm{T}}\in\underline{\mathscr{E}}$ remains stationary for all times and is therefore an equilibrium point of the PD-controlled system. Namely, if the inclusion $x_1^*\in(mg/k_1)[-\underline{\mu}, \underline{\mu}]$ holds, then it also holds that $x_1^*\in(mg/k_1)[-\mu(t), \mu(t)], \forall t$, due to Assumption 1. The time-varying nature of the stick set $\mathscr{E}(t)$ may, however, destroy the stationarity of points in $\mathscr{E}(t)\backslash\underline{\mathscr{E}}$. The set $\mathscr{E}(t)$ therefore denotes the stick set at time t and not an equilibrium set. The basic idea behind the impulsive controller (7), (8) and (9) is to apply an impulsive control force when the state of the system enters the maximal stick-set $\overline{\mathscr{E}}$. Loosely speaking, the impulsive force kicks the system out of the stick phase allowing it to further converge (closer) to the set-point. Since the friction law is uncertain also the stick set $\mathscr{E}(t)$ is not known *a priori* and the closed-loop system without impulsive control may even get stuck at zero velocity temporarily when $\mu(z, \dot{z}, t)$ is indeed time-dependent. To enforce that the system never remains at zero velocity for more than an isolated time instant (i.e. for a time interval of positive Lebesgue measure), we design the impulsive controller in (9) such that an impulsive force is applied whenever $\boldsymbol{x}^-(t)\in\overline{\mathscr{E}}$. Clearly, the impulsive part of the controller prevents the existence of an equilibrium set (and the occurrence of non-zero steady-state errors). However, energy will be added to the system at every time-instant on which an impulsive control action is applied. In this paper, we will provide design rules for k_1, k_2 and $k_3(x_1)$ such that more energy is dissipated (through the derivative action of the controller and the friction) in a time-interval between two impulsive control actions than is provided by the impulsive control action preceding this time-interval.

In order to design the impulsive part of the controller $k_3(x_1)$, we take the following perspective. Consider a time instant t_j for which $\boldsymbol{x}^-(t_j)\in\overline{\mathscr{E}}$, i.e. an impulsive control action $U=k_3(x_1(t_j))$ will be induced by the controller (7) at $t=t_j$. Note that an impulsive control force results only in a jump of the velocity $x_2(t)$ whereas the position $x_1(t)$ is absolutely continuous, as formalized in (13). The impulsive control action will cause $\boldsymbol{x}^+(t_j)\notin\overline{\mathscr{E}}$. Let t_{j+1} denote the first time-instant for which $\boldsymbol{x}(t)$ reaches again $\overline{\mathscr{E}}$, i.e. $x_2^-(t_{j+1})=0$. Now, we will design $k_3(x_1)$ in (9) such that the velocity will be reset to such a post-impact velocity $x_2^+(t_j)$ that the solution to (11), with $\mu(z, \dot{z}, t)=\underline{\mu}$ and initial condition $(x_1(t_j), x_2^+(t_j))$, will converge to the origin in finite time $\underline{t}_{j+1}$

DOI: 10.1002/rnc

without any impulses and/or velocity reversals occurring in the time-interval $(t_j, \underline{t}_{j+1}]$. So, the (impulsive) controller is designed such that it stabilizes the setpoint in finite time with only one impulsive action when the friction coefficient equals its lower bound. The impulsive controller design will satisfy the condition

$$k_3(y)=\begin{cases}<0, & y>0\\ =0, & y=0\\ >0, & y<0\end{cases}; \tag{23}$$

in other words, $\boldsymbol{x}=\mathbf{0}$ is an equilibrium point of the controlled system and the impulsive control force U is opposite to the position error $x_1(t_j)$, which appeals to our intuition. In Section 4, we will show that this control design also robustly stabilizes the closed-loop system with a time-varying and state-dependent friction coefficient $\mu(t)=\mu(x_1(t), x_2(t), t)$ satisfying Assumption 1.

Let us now design the impulsive control law $k_3(x_1)$ that has the above properties. Hereto, consider the case that $x_1(t_j)<0$ (the case $x_1(t_j)>0$ can be studied in an analogous fashion). This implies that $k_3(x_1(t_j))>0$, see (23), and $x_2^+(t_j)>0$. On the non-impulsive open time-interval $(t_j, \underline{t}_{j+1})$, the dynamics of (6) for $\mu(x_1, x_2, t)=\underline{\mu}$ is therefore governed by the differential Equation (15) with $\zeta>1$ and $f(t)=f_{\text{const}}=-g\underline{\mu}$, i.e.

$$\begin{aligned}\dot{\underline{x}}_1(t) &= \underline{x}_2(t)\\ \dot{\underline{x}}_2(t) &= -\omega_n^2\underline{x}_1(t)-2\zeta\omega_n\underline{x}_2(t)-g\underline{\mu}.\end{aligned} \tag{24}$$

We seek a solution curve of (24) with the boundary conditions $\underline{\boldsymbol{x}}^+(t_j)=[x_1(t_j) \quad x_2^+(t_j)]^{\mathrm{T}}$ and $\underline{\boldsymbol{x}}^-(\underline{t}_{j+1})=[0 \quad 0]^{\mathrm{T}}$. The initial position $x_1(t_j)$ and initial time t_j are *a priori* known. The initial velocity $x_2^+(t_j)$ as well as the end time $\underline{t}_{j+1}>t_j$ are yet unknown. We therefore have to solve a kind of mixed boundary value problem for the unknowns $x_2^+(t_j)$ and $\underline{t}_{j+1}$. The boundary value problem can be solved in many different ways. The rationale behind the method which we propose here is to arrive at an algebraic equation for which we can prove the existence and uniqueness of the solution. We can express the solution for $\mu(x_1, x_2, t)=\underline{\mu}$ in closed form using the general solution (19) by taking $\underline{t}_{j+1}=t_0$ as reference time and $x_{10}=\underline{x}_1(\underline{t}_{j+1})=0$, $x_{20}=x_2^-(\underline{t}_{j+1})=0$, which gives

$$\begin{aligned}\underline{x}_1(t) &= -\underline{c}(1-s_1(t-\underline{t}_{j+1}))=\underline{c}\left(\frac{\lambda_2}{\lambda_2-\lambda_1}\mathrm{e}^{\lambda_1(t-\underline{t}_{j+1})}-\frac{\lambda_1}{\lambda_2-\lambda_1}\mathrm{e}^{\lambda_2(t-\underline{t}_{j+1})}-1\right),\\ \underline{x}_2(t) &= -\lambda_1\lambda_2\underline{c}s_2(t-\underline{t}_{j+1})=\underline{c}\frac{\lambda_1\lambda_2}{\lambda_2-\lambda_1}(\mathrm{e}^{\lambda_1(t-\underline{t}_{j+1})}-\mathrm{e}^{\lambda_2(t-\underline{t}_{j+1})})\end{aligned} \tag{25}$$

with $\underline{c}$ given by (18).

Subsequently, using (25) we require that $\underline{x}_1(t)$ at time t_j equals the *a priori* known initial position $x_1(t_j)$. This yields a nonlinear real algebraic equation

$$\mathsf{f}(\underline{t}_{j+1})=0 \tag{26}$$

for the unknown end time $\underline{t}_{j+1}$, where the function $\mathsf{f}(t)$ is given by

$$\mathsf{f}(t):=\underline{c}(s_1(t_j-t)-1)-x_1(t_j)=\underline{c}\left(\frac{\lambda_2}{\lambda_2-\lambda_1}\mathrm{e}^{\lambda_1(t_j-t)}-\frac{\lambda_1}{\lambda_2-\lambda_1}\mathrm{e}^{\lambda_2(t_j-t)}-1\right)-x_1(t_j). \tag{27}$$

We can easily verify that $\mathsf{f}(t_j)=-x_1(t_j)>0$ holds.

Let us now study the following questions for the system of Equations (25)–(27):

- For which domain in $x_1(t_j)$ does a solution pair $(\underline{t}_{j+1}, x_2^+(t_j))$ exist (and can we show the uniqueness of this solution)?
- If such a solution pair exists, can we show that both the time lapse $\underline{t}_{j+1}-t_j$ and $x_2^+(t_j)$ are bounded for bounded $x_1(t_j)$ (i.e. the impulsive control law yields bounded impulses and the resulting flowing response of system (24) converges to the origin in finite time)?

DOI: 10.1002/rnc

In the following proposition, we propose the impulsive control law and show that it exhibits the above properties. Note that the impulsive control action $k_3(x_1(t_j))$ can be computed from (13) using the fact that $x_2^-(t_j)=0$:

$$k_3(x_1(t_j))=mx_2^+(t_j). \tag{28}$$

Proposition 2
Consider the impulsive control law $k_3(x_1(t_j))$ for a given $x_1(t_j)$, with t_j arbitrary, defined by (28), where

1. $\underline{t}_{j+1}$ is the solution of (26) and (27);
2. the value of $x_2^+(t_j)$ is determined by the evaluation of $\underline{x}_2(t)$, given by (25) at $t=t_j$.

If $\zeta>1$, then it holds that $k_3(x_1)$ is uniquely defined and bounded for all $(x_1,x_2)\in\overline{\mathscr{E}}$.

Proof
The proof is given in Appendix A. □

Note that the impulsive control law (28) can be computed *a priori* given the plant properties, such as the mass m, the uncertainty bounds $\underline{\mu}$ and $\overline{\mu}$ on the friction coefficient, the gains k_1 and k_2 of the PD-controller and the gravitational acceleration g.

3.2.1. Characteristics of the impulsive control law. In this section, we further illuminate particular characteristics of the impulsive control law $k_3(x_1)$ designed above. These characteristics will be exploited in Section 4 to study the stability of the impulsive closed-loop system.

It holds that $x_2^+(t_j)=-\mathsf{f}'(\underline{t}_{j+1})$ and we can therefore write $\mathrm{d}x_2^+(t_j)/\mathrm{d}\underline{t}_{j+1}=-\mathsf{f}''(\underline{t}_{j+1})$. Moreover, differentiation of the algebraic equation $\mathsf{f}(\underline{t}_{j+1};x_1(t_j))=0$, in which with some abuse of notation we make explicit that f also depends on $x_1(t_j)$, using $\partial\mathsf{f}/\partial x_1(t_j)=-1$, yields

$$\mathsf{f}'(\underline{t}_{j+1})\,\mathrm{d}\underline{t}_{j+1}-\mathrm{d}x_1(t_j)=0\Longrightarrow\frac{\mathrm{d}\underline{t}_{j+1}}{\mathrm{d}x_1(t_j)}=\frac{1}{\mathsf{f}'(\underline{t}_{j+1})}. \tag{29}$$

Consequently, the impulsive control law $k_3(x_1(t_j))$ has a slope given by

$$\frac{\mathrm{d}k_3(x_1(t_j))}{\mathrm{d}x_1(t_j)}=m\frac{\mathrm{d}x_2^+(t_j)}{\mathrm{d}x_1(t_j)}=m\frac{\mathrm{d}x_2^+(t_j)}{\mathrm{d}\underline{t}_{j+1}}\frac{\mathrm{d}\underline{t}_{j+1}}{\mathrm{d}x_1(t_j)}=-m\frac{\mathsf{f}''(\underline{t}_{j+1})}{\mathsf{f}'(\underline{t}_{j+1})}, \tag{30}$$

or, using $\mathsf{f}'(\underline{t}_{j+1})=-x_2^+(t_j)=-k_3(x_1(t_j))/m$, by $k_3'(x_1(t_j))=m^2(\mathsf{f}''(\underline{t}_{j+1})/k_3(x_1(t_j)))$. For $\zeta>1$, it holds that $\mathsf{f}''(\underline{t}_{j+1})\leqslant-\underline{c}\omega_n^2-\lambda_2\mathsf{f}'(\underline{t}_{j+1})$ for all $\underline{t}_{j+1}\geqslant t_j$. We therefore obtain the differential inequality

$$k_3'(y)\leqslant m\lambda_2-\frac{\underline{c}\omega_n^2m^2}{k_3(y)}, \tag{31}$$

on the domain $y<0$ with the boundary condition $k_3(0)=0$. The differential equation $h'=-a/h$ with $h(0)=0$ has the solution $h(x)=\sqrt{-2ax}$ on the domain $x\leqslant0$. The impulsive control law $k_3(y)$ is therefore bounded from below by

$$k_3(y)\geqslant\sqrt{-2\underline{c}\omega_n^2m^2y},\quad y\leqslant0, \tag{32}$$

as well as by

$$k_3(y)\geqslant m\lambda_2y\quad\text{for } y\leqslant0. \tag{33}$$

The symmetry of the problem implies the unevenness of $k_3(y)$, i.e. $k_3(y)=-k_3(-y)$, and we therefore obtain

$$k_3(y)\leqslant-\sqrt{2\underline{c}\omega_n^2m^2y},\quad y\geqslant0. \tag{34}$$

DOI: 10.1002/rnc

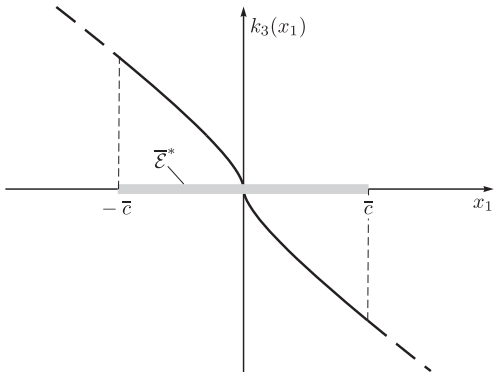

Figure 2. Schematic representation of the impulsive control law $k_3(x_1)$ for $\zeta \geqslant 1$ ($\overline{\mathscr{E}}^* = \{\boldsymbol{x}_1 \in \mathbb{R} \,|\, |x_1| \leqslant (mg\overline{\mu}/k_1)\}$).

Moreover, for small values of $|y|$ the impulsive control law $k_3(y)$ can be well approximated by

$$k_{3\text{approx}}(y) = -\operatorname{sign}(y)\sqrt{2\underline{c}\omega_n^2 m^2 |y|} \tag{35}$$

because if $y \uparrow 0$ then $\underline{t}_{j+1} \downarrow t_j$ and $\mathsf{f}''(\underline{t}_{j+1}) \uparrow -\underline{c}\omega_n^2$. Hence if $\zeta > 1$, then the slope $k_3'(y)$ is negative for all $y \neq 0$, but is tending to minus infinity for $y \to 0$. The graph of the impulsive control law $k_3(y)$, which is a continuous uneven function, is therefore strictly decreasing for $\zeta > 1$ and is locally similar to the square-root function $k_{3\text{approx}}(y)$ around the origin. A schematic representation of the impulsive control law $k_3(x_1)$ for $\zeta > 1$ is given in Figure 2, where we recall that it is only applied for $x_1 \in \overline{\mathscr{E}}^* = \{\boldsymbol{x}_1 \in \mathbb{R} \,|\, |x_1| \leqslant (mg\overline{\mu}/k_1)\}$ (the solid part of the graph).

The characteristics of the impulsive control explicated in (32), (34) and (35) will be used in Proposition 6, which, in turn, plays a key role in the stability analysis in Section 4.

3.3. Switching impulsive controller design

We will consider the following switching impulsive control law consisting of three phases:

1. The system starts at an arbitrary initial condition $\boldsymbol{x}(t_0) \in \mathbb{R}^2$. The parameters k_1 and k_2 of the PD-controller are chosen such that the closed loop system without friction is an undercritically damped oscillator (i.e. $\zeta < 1$). We assume that the solution $\boldsymbol{x}(t)$ is attracted in a finite time (denoted by t_1) to $\overline{\mathscr{E}}$. In the next section, we will formalize this assumption and provide sufficient conditions under which this assumption is satisfied, which will explicate the motivation for the choice of $\zeta < 1$ in ensuring finite-time attractivity to the stick-set.
2. The impulsive controller turns on at $t = t_1 \geqslant t_0$ when $\boldsymbol{x}^-(t_1) \in \overline{\mathscr{E}}$ and the k_2 parameter of the PD controller is increased, such that $\zeta > 1$. We opt for tuning k_2 (for $t \geqslant t_1$) such that $\zeta > 1$ for the following reasons. First, certain key characteristics of the impulsive control law, see Proposition 2 and Section 3.2.1, have been proven for $\zeta > 1$. Second, choosing $\zeta > 1$ (actually choosing ζ large) is desirable from a transient performance perspective (this statement will be supported by simulations in Section 5, see Figure 9). Third, we will show in Section 5 that the proposed impulsive control law will guarantee the global uniform symptotic stability of the set-point for an arbitrarily large uncertainty in the friction coefficient by choosing ζ sufficiently large, see Assumption 3 and Remark 3.
   The impulsive controller induces a velocity jump to $x_2^+(t_1)$ such that the following non-impulsive motion results in
   (a) $\boldsymbol{x}^-(t_2) = \boldsymbol{0}$ if $\mu(t) = \underline{\mu}$, which defines the value of $x_2^+(t_1)$ and therefore the impulsive control action $k_3(x_1(\overline{t}_1))$, see Section 3.2,

DOI: 10.1002/rnc

(b) $\underline{\boldsymbol{x}}^-(t_2) \in \underline{\mathscr{E}}$ for arbitrary $\mu(t)$, which puts an additional condition on $\overline{\mu}$ and μ, see Assumption 3 in Section 4, which can, however, always be satisfied by choosing $\overline{\zeta}$ large enough.

We will prove that t_2 is finite, see Proposition 7 in Section 4.

3. The impulsive control is applied at each time-instant t_j for which $\boldsymbol{x}^-(t_j) \in \overline{\mathscr{E}}$. It holds that $\boldsymbol{x}^-(t_2) \in \underline{\mathscr{E}}$ and the control is such that $\boldsymbol{x}^-(t_j) \in \underline{\mathscr{E}}$, $j = 2, 3, \ldots$. Infinitely many impulsive actions will occur in a finite time, i.e. $t_\infty < \infty$, with $\boldsymbol{x}(t_\infty) = \boldsymbol{0}$, see Proposition 10 in Section 4.

The resulting switching impulsive control law is now given by (7), (9) and

$$u(x_1, x_2, t) = -k_1 x_1 - k_2(t) x_2, \quad k_1, k_2 > 0,$$
$$k_2(t) = \begin{cases} k_{21} & \text{for } t_0 \leqslant t < t_1 \\ k_{22} & \text{for } t \geqslant t_1 \end{cases}, \tag{36}$$

such that $k_1 > 0$, $0 < k_{21}/(2\sqrt{k_1 m}) < 1$ and $k_{22}/(2\sqrt{k_1 m}) > 1$, and where t_1 is the smallest time instant $t_1 \geqslant t_0$ such that $\boldsymbol{x}^-(t_1) \in \overline{\mathscr{E}}$.

4. STABILITY ANALYSIS

In the previous section, we have introduced the switching impulsive control design. In this section, we will show that this control design symptotically (finite-time) stabilizes the set-point $\boldsymbol{x} = \boldsymbol{0}$. Consider the system (6) satisfying Assumption 1 and the impulsive feedback controller (7), (9) and (36) with $k_3(x_1)$ satisfying (28) and $x_2^+(t_j)$ fulfilling the mixed boundary value problem (see point 2 in Proposition 2). In the following we will call this the resulting closed-loop system. We will prove that $\boldsymbol{x} = \boldsymbol{0}$ is a globally uniformly symptotically stable equilibrium point of the resulting closed-loop system.

Let us first prove boundedness of solutions.

Proposition 3
The solutions of the resulting closed-loop system (6), (7), (9) and (36), satisfying Assumption 1, are bounded.

Proof
The proof is given in Appendix A. □

Second, let us assume that solutions, which start in $\boldsymbol{x}(t_0) \in \mathbb{R}^2$, reach the compact set $\overline{\mathscr{E}}$ in a finite time t_1.

Assumption 2
Solutions of the resulting closed-loop system (6), (7), (9) and (36), satisfying Assumption 1, which start at $\boldsymbol{x}(t_0) \in \mathbb{R}^2$ reach the compact set $\overline{\mathscr{E}}$ in a finite time t_1 (i.e. $t_1 - t_0 < \infty$).

We now formulate two sufficient conditions for Assumption 2 in the following two propositions.

Proposition 4
Suppose the friction coefficient $\mu(x_1, x_2, t)$ satisfies Assumption 1. If the time-evolution of the friction coefficient $\mu(t) = \mu(x_1(t), x_2(t), t)$ along solutions of the closed-loop system (6), (7), (36), with $U = 0$, is piecewise constant, such that it is constant during each time-interval for which $x_2(t)$ does not change sign, and the linear part of the closed loop system is undercritically damped (i.e. $\zeta < 1$), then the stick set $\overline{\mathscr{E}}$ is reached in finite time for any initial condition $\boldsymbol{x}(t_0) \in \mathbb{R}^2$.

Proof
In [34], Theorem 2(iii), finite-time attraction is proven for a constant value of $\mu(t)$. The proof can easily be extended to a piecewise constant $\mu(t)$ as in the proposition. □

DOI: 10.1002/rnc

Proposition 5
Consider the closed-loop system (6), (7), (36), with $U=0$. Consider a velocity-dependent friction laws satisfying the decomposition $F_f(x_2)\in -mg\mu\,\mathrm{Sign}(x_2)-F_{sm}(x_2)$ instead of the friction law in (3), where μ is constant and satisfies Assumption 1, $F_{sm}(\cdot)\in\mathscr{C}^1$ and $F_f(x_2)x_2\leqslant 0, \forall x_2$. If

$$k_{21}+\frac{\partial F_{sm}}{\partial x_2}(0)<2\sqrt{mk_1}, \tag{37}$$

i.e. the linearization of the continuous part of the closed-loop dynamics (around the origin) is undercritically damped, then the stick set $\overline{\mathscr{E}}$ is reached in finite time for any initial condition $\boldsymbol{x}(t_0)\in\mathbb{R}^2$.

Proof
Under the conditions in the proposition, Theorem 2 in [34] can be directly employed to provide the proof. □

Remark 1
Given the rather generic class of friction laws considered in this paper, the conditions on the friction law in Propositions 4 and 5 can be considered to be restrictive. Note, however, that (possibly asymmetric) Coulomb friction laws with uncertain (though constant) friction coefficient form a practically relevant subclass of friction models that satisfies the conditions in Proposition 4 and that the friction law in Proposition 5 represents a general class of discontinuous, velocity-dependent friction laws (possibly including the Stribeck effect). Moreover, the formulation of less stringent conditions for the finite-time convergence to the stickset for the case of generic friction coefficients $\mu(x_1,x_2,t)$ is, to the best the authors' knowledge, an open problem. Namely, it has been shown in [34, 35] that, even for constant μ, manifolds in state space may exist for which solutions only converge to the equilibrium set asymptotically (not in finite time). More precisely, in [34], it is shown that under the conditions in Proposition 5 with $k_{21}+(\partial F_{sm}/\partial x_2)(0)\geqslant 2\sqrt{mk_1}$, solutions exist that reach the equilibrium set in infinite time. Based on Propositions 4 and 5 and the work in [34, 35], we conclude that the fact that the linearized dynamics is undercritically damped appears to be an essential condition for the finite-time attractivity of the equilibrium set. This is the reason for designing the switching controller as in (36).

We do stress here that, although more generic sufficient conditions for Assumption 2 are currently lacking, it has been widely observed in the literature (both on a model level as in experiments), see e.g. [3, 7, 8], that solutions in practice generally do converge to the stickset in finite time. In fact, this finite-time convergence to the stick set is directly related to the problems of stick-slip limit cycling and non-zero steady-state errors, which we are aiming to tackle with the control design in this paper and form the core motivation for our work. Hence, from a practical point of view, Assumption 2 is a very natural one.

Remark 2
Let us consider an alternative tuning for the switching state-feedback controller in (36) such that also the position feedback gain is switched according to $k_1=0$, for $t_0\leqslant t\leqslant t_1$, $k_1\leqslant mg\overline{\mu}/|x_1(t_1)|$, for $t\geqslant t_1$ and the velocity feedback gain $k_2>0$ is taken constant and such that $\zeta>1$ for $t\geqslant t_1$. In this case it is straightforward to show that for general $\mu(x_1,x_2,t)$, satisfying Assumption 1, Assumption 2 is satisfied. Still, we prefer to use the design proposed in (36) since the above alternative control design leads to position feedback gains dependent on the initial conditions, which may lead to unpredictable/inferior transient performance.

Using the arguments and assumptions above we can now consider initial conditions (at $t=t_1$) satisfying $\boldsymbol{x}^-(t_1)=[x_1(t_1)x_2^-(t_1)]^{\mathrm{T}}\in\overline{\mathscr{E}}^-:=\{\boldsymbol{x}\in\overline{\mathscr{E}}\,|\,x_1<0\}$. The case in which $x_1>0$ can be treated in an entirely analogous fashion. Now, we consider a sequence of time instants t_j, $j\geqslant 1$, such that $\boldsymbol{x}^-(t_j)\in\overline{\mathscr{E}}^-$ and $\boldsymbol{x}(t)\notin\overline{\mathscr{E}}^-$ for $t\neq t_j$. Clearly, due to the design of the impulsive part of the control law as in (9), an impulse will now be applied instantly at $t=t_j$ and the system undergoes a state reset to $\boldsymbol{x}^+(t_j)=[x_1(t_j)\ \ x_2^+(t_j)]^{\mathrm{T}}=[x_1(t_j)\ \ k_3(x_1(t_j))/m]^{\mathrm{T}}$, see (13). We will show below

DOI: 10.1002/rnc

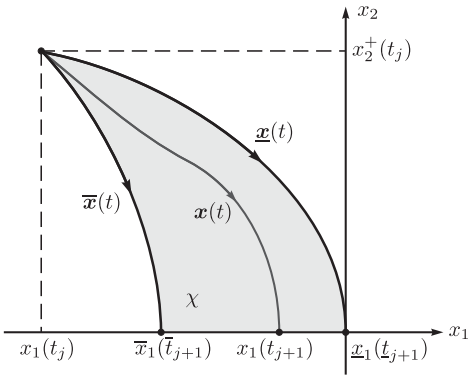

Figure 3. Graphical representation of several solutions of the closed-loop system between two control impulses (for the case that $x_1(t_j)<0$).

that if $x_1(t_1)<0$, then $x_1(t_j)\leqslant 0, \forall j\geqslant 1$. Note that for $x_1(t_j)<0$ we have that $x_2^+(t_1)>0$, since $x_1(t_j)k_3(x_1(t_j))<0$. Now, we study solutions flowing from $\boldsymbol{x}^+(t_j)$ until they reach again the set $\overline{\mathscr{E}}$. We denote the next time instants at which these solutions reach $\overline{\mathscr{E}}$ by t_{j+1}, $\underline{t}_{j+1}$ and $\overline{t}_{j+1}$ for $\mu=\mu(x_1,x_2,t)$, $\mu=\underline{\mu}$ and $\mu=\overline{\mu}$, respectively. In doing so, we consider three different systems:

1. System (15) with $f(t)=-g\mu(x_1(t),x_2(t),t)$ and solution $\boldsymbol{x}(t)$ on (t_j,t_{j+1}),
2. System (15) with $f(t)=-g\underline{\mu}$, i.e. system (24), and solution $\underline{\boldsymbol{x}}(t)$ on $(t_j,\underline{t}_{j+1})$,
3. System (15) with $f(t)=-g\overline{\mu}$ and solution $\overline{\boldsymbol{x}}(t)$ on $(t_j,\overline{t}_{j+1})$.

All three solutions $\boldsymbol{x}(t)$, $\underline{\boldsymbol{x}}(t)$ and $\overline{\boldsymbol{x}}(t)$ have the same initial condition and are sketched in Figure 3. By $\Gamma_{\underline{\mu}}$ we denote the solution segment $\underline{\boldsymbol{x}}(t)$, for $t\in(t_j,\underline{t}_{j+1})$, and by $\Gamma_{\overline{\mu}}$ we denote the solution segment $\overline{\boldsymbol{x}}(t)$, for $t\in(t_j,\overline{t}_{j+1})$. By χ we denote the set enclosed by the line segments $\Gamma_{\underline{\mu}}$, $\Gamma_{\overline{\mu}}$ and the axis $x_2=0$ (gray set in Figure 3). A solution $\boldsymbol{x}(t)$ which starts in the set χ cannot cross $\Gamma_{\underline{\mu}}$ or $\Gamma_{\overline{\mu}}$. So, the solution $\boldsymbol{x}(t)$ is confined between $\Gamma_{\underline{\mu}}$ and $\Gamma_{\overline{\mu}}$ and if it leaves χ then this can only happen through the line $x_2=0$. However, for an arbitrary initial condition, it might also be that the solution approaches the edge of $\mathscr{E}(t)$ asymptotically and therefore never leaves χ (we once more recall the results in [34, 35]). We first show that for $\mu(t)=\overline{\mu}$ solutions which start in $\overline{\mathscr{E}}$ return to $\overline{\mathscr{E}}$ in a finite time and that this return is governed by a contraction map.

Proposition 6
The flow of the resulting closed-loop system (6), (7), (9) and (36) with $\mu(t)=\overline{\mu}$ maps initial conditions $\overline{\boldsymbol{x}}^-(\overline{t}_j)\in\overline{\mathscr{E}}$ to $\overline{\boldsymbol{x}}^-(\overline{t}_{j+1})\in\overline{\mathscr{E}}$, such that

$$y_{j+1}=\overline{F}(y_j), \tag{38}$$

with $y_j=\overline{x}_1(\overline{t}_j)$, is a contraction map.

Proof
The proof is given in Appendix A. □

We now return to the problem that a solution $\boldsymbol{x}^+(t_j)$ is confined to the set χ, but (if no additional assumptions are made) might approach the end of the stick set $\mathscr{E}(t)$ asymptotically and might therefore not return to $\boldsymbol{x}^-(t_{j+1})\in\mathscr{E}$ in a finite time $t_{j+1}<\infty$. To avoid such undesirable behavior, we adopt the following assumption.

Assumption 3
We assume that one of the following two conditions holds:

$$\underline{\mu}/\overline{\mu}>\tfrac{1}{2}, \tag{39}$$

DOI: 10.1002/rnc

or

$$\underline{\mu}/\overline{\mu}>1-\left(\frac{\lambda_1}{\lambda_2}\right)^{-a_1}, \tag{40}$$

where $a_1=-(\lambda_1/(\lambda_2-\lambda_1))$, and λ_1 and λ_2 defined in (16).

Under this assumption it holds that the previously defined map $\overline{F}$ in (38) satisfies $\overline{F}(-\overline{c})\geqslant(1-\underline{\mu}/\overline{\mu})\cdot(-\overline{c})>-\underline{c}$. This assumption restricts the $\Gamma_{\overline{\mu}}$ border of χ to end in $\underline{\mathscr{E}}$. This fact will, in turn, be used to show that solutions of the resulting closed-loop system with time-varying $\mu(t)$ return in finite time to $\underline{\mathscr{E}}$.

Proposition 7
A solution of the resulting closed-loop system (6), (7), (9) and (36), satisfying Assumptions 1 and 3, which starts in $\overline{\mathscr{E}}$ at $t=t_1$, returns to $\underline{\mathscr{E}}$ in a finite time interval t_2-t_1.

Proof
The proof is given in Appendix A. □

Remark 3
We note that the condition (40) in Assumption 3 can always be satisfied by choosing $\zeta=k_{22}/(2\sqrt{k_1 m})>1$ large enough. Namely, it holds that, first, the function $1-(\lambda_1/\lambda_2)^{-a_1}$ is strictly decreasing for increasing ζ (for $\zeta>1$) and, second, $\lim_{\zeta\to\infty}1-(\lambda_1/\lambda_2)^{-a_1}=0$. To validate the latter statement, recall from (16) that $\lambda_1:=-\omega_n\zeta+\omega_n\sqrt{\zeta^2-1}$, $\lambda_2:=-\omega_n\zeta-\omega_n\sqrt{\zeta^2-1}$ and $a_1=-(\lambda_1/(\lambda_2-\lambda_1))$ and define $q:=\lambda_1/\lambda_2$, $p:=1-q$. Using these definitions we can derive that $\lim_{\zeta\to\infty}1-(\lambda_1/\lambda_2)^{-a_1}=\lim_{q\downarrow 0}(1-q^{q/(1-q)})=1-\lim_{q\downarrow 0}q^q=1-\lim_{q\downarrow 0}\mathrm{e}^{q\ln q}=0$. We stress here that this fact will allow us to guarantee robust stability for any uncertainty level in the friction by designing the non-impulsive part of the controller such that ζ is large enough (satisfying condition (40)).

Still, we care to also provide condition (39) ($\underline{\mu}/\overline{\mu}>\frac{1}{2}$) in Assumption 3, which is independent of ζ, since this condition is less strict than condition (40) for ζ close to 1. Namely, $\lim_{\zeta\downarrow 1}1-(\lambda_1/\lambda_2)^{-a_1}=\lim_{q\uparrow 1}(1-q^{q/(1-q)})=\lim_{p\downarrow 0}(1-(1-p)^{(1-p)/p})=1-\lim_{p\downarrow 0}\mathrm{e}^{((1-p)/p)\ln(1-p)}=1-(1/e)\approx 0.63>\frac{1}{2}$.

Next, we consider the impulse times t_j with $j>2$ and $\boldsymbol{x}^-(t_2)\in\underline{\mathscr{E}}$. We prove that if $\boldsymbol{x}^-(t_2)\in\underline{\mathscr{E}}^-$ then it holds that $\boldsymbol{x}^-(t_j)\in\underline{\mathscr{E}}^-$ for all $j>2$. Similar reasoning holds for $\boldsymbol{x}^-(t_2)\in\underline{\mathscr{E}}^+$ due to the symmetry properties of the system.

Proposition 8
Solutions of the resulting closed-loop system (6), (7), (9) and (36) with a friction coefficient $\mu(x_1,x_2,t)$, satisfying Assumption 1, which start in $\underline{\mathscr{E}}^-$ at $t=t_j$ return to $\underline{\mathscr{E}}^-$ in a finite time $t_{j+1}-t_j$ with the lower and upper bounds $\overline{t}_{j+1}\leqslant t_{j+1}\leqslant\underline{t}_{j+1}$ given by

$$\overline{t}_{j+1}-t_j=\frac{1}{\lambda_2-\lambda_1}\ln\left(\frac{-\lambda_1\lambda_2(x_1(t_j)+\overline{c})+\lambda_1 x_2^+(t_j)}{-\lambda_1\lambda_2(x_1(t_j)+\overline{c})+\lambda_2 x_2^+(t_j)}\right), \tag{41}$$

$$\underline{t}_{j+1}-t_j=\frac{1}{\lambda_2-\lambda_1}\ln\left(\frac{-\lambda_1\lambda_2(x_1(t_j)+\underline{c})+\lambda_1 x_2^+(t_j)}{-\lambda_1\lambda_2(x_1(t_j)+\underline{c})+\lambda_2 x_2^+(t_j)}\right), \tag{42}$$

with $\overline{x}_1(\overline{t}_{j+1})\leqslant x_1(t_{j+1})\leqslant\underline{x}_1(\underline{t}_{j+1})=0$.

Proof
The proof is given in Appendix A. □

We conclude that if $\boldsymbol{x}^-(t_j)\in\underline{\mathscr{E}}$, then the solution $\boldsymbol{x}(t)\in\chi$ for $t\in(t_j,t_{j+1})$ and that this solution will hit the line $x_2=0$ in finite time-lapse $t_{j+1}-t_j$ with lower and upper bound given by (41)

DOI: 10.1002/rnc

and (42), respectively. Note that, due to Proposition 2, we have that $x_2(t_j^+)=mk_3(x_1(t_j))$ is bounded and, consequently, both $\underline{t}_{j+1}$ and $\overline{t}_{j+1}$ are upper bounded, which also follows from (A13). In other words, after an impulsive control action a finite time interval of smooth flow follows before the next control impulse is applied.

Next, we exploit Proposition 8, which states that the position errors $y_j=x_1(t_j)$ at the impulse times t_j converge to zero faster for system (11) with time-varying $\mu(t)$ than for system (11) with $\mu(t)=\overline{\mu}$. Note that Proposition 8 only holds for initial conditions in $\underline{\mathscr{E}}$.

Proposition 9
The flow of the resulting closed-loop system (6), (7), (9) and (36) with a friction coefficient $\mu(x_1,x_2,t)$, satisfying Assumption 1, maps initial conditions $\boldsymbol{x}^-(t_j)\in\underline{\mathscr{E}}$ to $\boldsymbol{x}^-(t_{j+1})\in\underline{\mathscr{E}}$, such that

$$y_{j+1}=F(y_j), \tag{43}$$

with $y_j=x_1(t_j)$, is a contraction map.

Proof
Proposition 8 proves that if $-\underline{c}\leqslant y_j\leqslant 0$, then it holds that $\overline{F}(y_j)\leqslant F(y_j)\leqslant 0$. Proposition 6 proves that $\overline{F}$ is a contraction map, hence the map F is also a contraction map within $\underline{\mathscr{E}}$. □

Proposition 9 proves that the sequence $y_j=x_1(t_j)$ converges to zero (i.e. the positioning error at the impulse times converges to zero). Next, we show that the position error converges to zero in *finite time*.

Proposition 10
A solution of the resulting closed-loop system (6), (7), (9) and (36) with a friction coefficient $\mu(x_1,x_2,t)$, satisfying Assumption 1, and initial condition $\boldsymbol{x}^-(t_2)\in\underline{\mathscr{E}}$ reaches the origin in a finite time

$$t_\infty-t_2\leqslant\sqrt{\frac{2|y_2|}{g\underline{\mu}}}\frac{1}{1-\left(1-\frac{\underline{\mu}}{\overline{\mu}}\right)^{1/2}}, \tag{44}$$

with $y_2=x_1(t_2)$ and $\boldsymbol{x}(t_\infty)=\boldsymbol{0}$.

Proof
The proof is given in Appendix A. □

Proposition 11
Consider the resulting closed-loop system (6), (7), (9) and (36) satisfying Assumptions 1, 2 and 3. The solutions of the resulting closed-loop system are bounded and converge to $\boldsymbol{x}=\boldsymbol{0}$ in a finite time.

Proof
Boundedness is proven in Proposition 3. Assumption 2 assures that a solution with an arbitrary initial condition $\boldsymbol{x}(t_0)\in\mathbb{R}^2$ reaches $\overline{\mathscr{E}}$ is a finite time t_1. Under Assumption 3, Proposition 7 proves that any solution of the resulting closed-loop system which starts in $\overline{\mathscr{E}}$ at $t=t_1$ returns to $\underline{\mathscr{E}}$ in a finite time t_2. Propositions 9 and 10 prove that a solution which starts in $\boldsymbol{x}^-(t_2)\in\underline{\mathscr{E}}$ reaches the origin in a finite time. □

Finally, we will show that the origin of the resulting closed-loop system is globally uniformly symptotically stable.

Theorem 1
Consider the resulting closed loop system (6), (7), (9) and (36) satisfying Assumptions 1, 2 and 3. The origin of the resulting closed-loop system is globally uniformly symptotically stable.

Proof
The proof is given in Appendix A. □

DOI: 10.1002/rnc

We note that Theorem 1 states that the proposed impulsive control law can render the set-point globally uniformly symptotically stable for a very wide class of friction models. Namely, Assumption 1 only requires the friction coefficient to be bounded from above (and below) and Assumption 3 can be satisfied for any level of uncertainty in the friction by appropriately tuning the non-impulsive part of the controller (i.e. by taking $\zeta = k_{22}/(2\sqrt{k_1 m})$ large enough).

Remark 4

In practice, one may not be able to induce infinitely many impulsive actuation forces in a finite time interval. In such a case, one could resort to artificially delaying the impulses once the response gets stuck in the minimal stick set $\underline{\mathscr{E}}$ such that always a finite (small) time interval between impulses is guaranteed. Then, the resulting closed-loop response in the phase space will remain unchanged (with respect to the case with undelayed impulses) and hence the response will still converge to the set-point. However, only *asymptotic* stability can now be guaranteed (as opposed to finite-time convergence to the set-point).

5. ILLUSTRATIVE EXAMPLE

In this section, we illustrate the effectiveness of the impulsive control strategy, developed in this paper, by means of an example. Hereto, we consider a motion system as in Figure 1 with dynamics described by (6), where the inertia is taken to be $m = 1$ and the gravitational acceleration $g = 10$. Moreover, the friction coefficient in (6) is of the form $\mu(x_1, x_2, t) = (\mu_1 - \mu_2)/(1 + 0.5|x_2|) + \mu_2 + \mu_3 \sin(\Omega t)$, where $\mu_1 = 0.4$, $\mu_2 = 0.3$, $\mu_3 = 0.05$ and $\Omega = 4$. In this friction law one can recognize a velocity-dependency with a pronounced Stribeck effect and an explicit time-dependency. Note that this friction law satisfies Assumption 1 with $\underline{\mu} = 0.25$ and $\overline{\mu} = 0.45$, which indicates a significant possible variation on the friction coefficient and which also implies the satisfaction of Assumption 3. The possible variation of the friction coefficient is also illustrated by the dashed lines in Figure 4. Next, we employ the switching impulsive controller design proposed in Section 3 and described by (7), (9) and (36). Herein, the control parameters are designed as $k_1 = 1$, $k_{21} = 0.5$, $k_{22} = 3$, implying that $0 < k_{21}/(2\sqrt{k_1 m}) = 0.25 < 1$ and $k_{22}/(2\sqrt{k_1 m}) = 1.5 > 1$ as proposed in Section 3.3, and the impulsive control design (9) is designed as depicted in Figure 5, where $k_3(y) = K_3(y)$ since $m = 1$.

We employ a numerical time-stepping scheme [30, 31, 36] to numerically compute solutions of the impulsive closed-loop system. Figures 6 and 7 depict a simulated response of the closed-loop

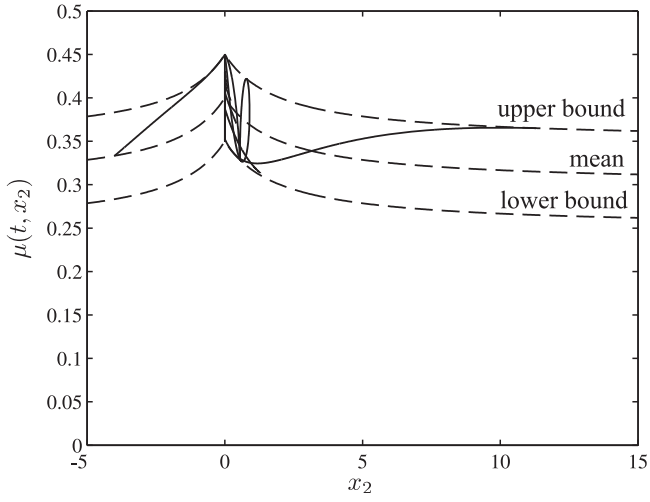

Figure 4. Friction coefficient. Dashed lines indicate bounds on and mean of the friction coefficient and the solid line indicates the evolution of the friction coefficient along a solution of the closed-loop system.

DOI: 10.1002/rnc

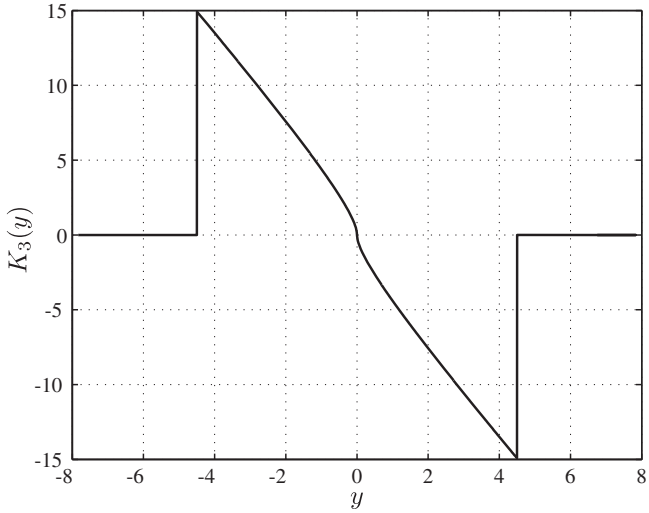

Figure 5. Impulsive control law.

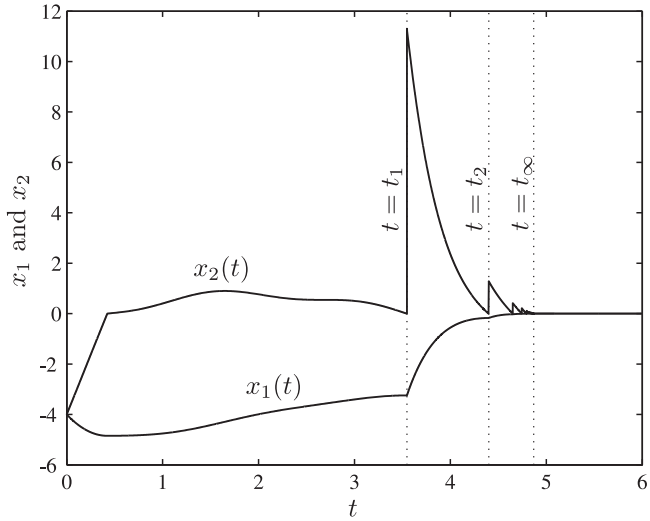

Figure 6. Time history of the position $x_1(t)$ and the velocity $x_2(t)$ for $x_1(0) = -4$ and $x_2(0) = -4$.

system for an initial condition $x_1(0) = -4$ and $x_2(0) = -4$. Figure 8 shows the corresponding time evolution of the friction coefficient along this solution of the closed-loop system (a different perspective on the variation of the friction coefficient along the same solution of the closed-loop system is represented by the solid line in Figure 4). Figure 6 clearly shows that the response indeed converges to the origin in finite time, while the jumps in the velocity induced by the impulsive control action are clearly visible. This figure also displays the time instants $t_1 = 3.55$ and $t_2 = 4.40$ at which the response hits, for the first time, the sets $\overline{\mathscr{E}}$ (maximal stick set) and $\underline{\mathscr{E}}$ (minimal stick set), respectively (see also Figure 7). Moreover, the response converges to the origin in the finite time $t_\infty = 4.8707$. The upper bound on t_∞ that can be computed using Proposition 10 is $t_\infty = 5.5162$. This upper bound on t_∞ is not overly conservative and can be considered to be a realistic bound on the time in which convergence to the setpoint is achieved.

Next, we investigate the influence of the tuning of the parameter $\zeta = k_{22}/(2\sqrt{k_1 m})$ (for $t \geqslant t_1$) of the non-impulsive part of the controller on the transient performance of the closed-loop system. Thereto, simulations have been performed for the same parameter settings and initial condition as above, however, for a range of values for $\zeta > 1$ (which has been attained by varying the

DOI: 10.1002/rnc

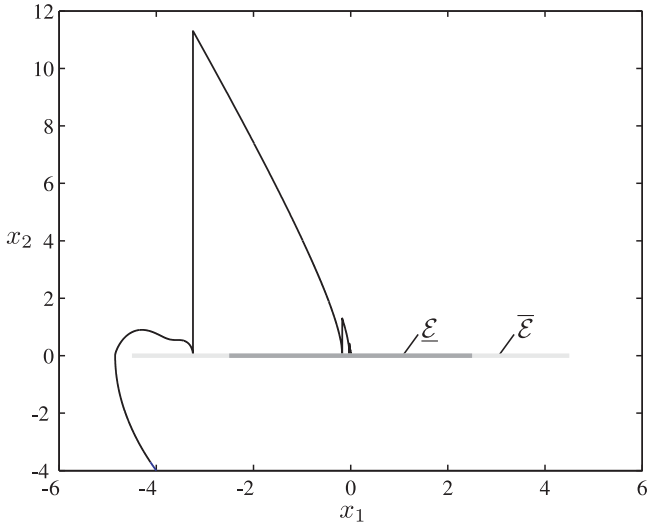

Figure 7. Phase portrait depicting $x_2(t)$ versus $x_1(t)$ for $x_1(0) = -4$ and $x_2(0) = -4$.

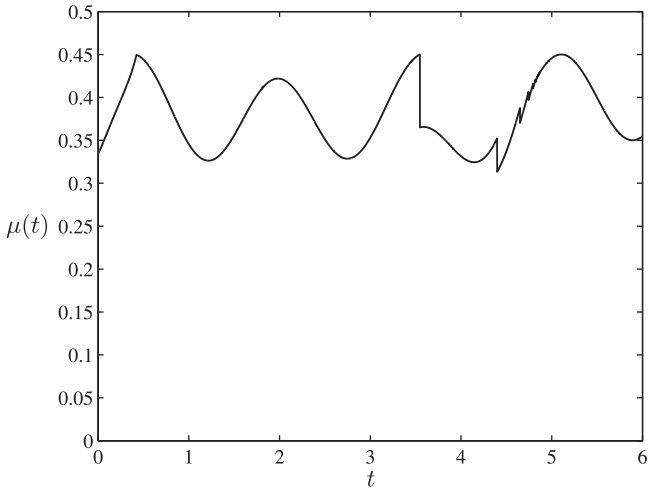

Figure 8. Time evolution of the friction coefficient along a solution of the closed-loop system for $x_1(0) = -4$ and $x_2(0) = -4$.

parameter k_{22}). Figure 9 shows the results of these simulations in terms of the time lapse $t_\infty - t_1$ and shows that the convergence of the system to the set-point becomes faster for larger values of ζ (note that t_1 is the same for all simulations since identical initial conditions are used).

Figures 10 and 11 depict a simulated response of the closed-loop system for an initial condition $x_1(0) = -4$ and $x_2(0) = -4$ for the case of 10% uncertainty on the mass m (all the other parameters are unchanged). More specifically, the value of the real mass is as above ($m = 1$), while the mass used in the design of the impulsive control law is $m = 1.1$. Figures 10 and 11 show that due to the uncertainty in the mass the closed-loop response exhibits some overshoot and $t_\infty = 4.9235$ is slightly larger than in the case of no uncertainty ($t_\infty = 4.8707$). However, despite the uncertainty in the mass the impulsive controller still robustly stabilizes the set-point in finite time. This simulation shows that the control design is robust against (small) model uncertainties.

We care to stress that the impulsive control design by no means exploits knowledge on the particular friction law used in this example and indeed guarantees *robust stabilization* for any position-, velocity- and time-dependent friction coefficient satisfying the same bounds.

DOI: 10.1002/rnc

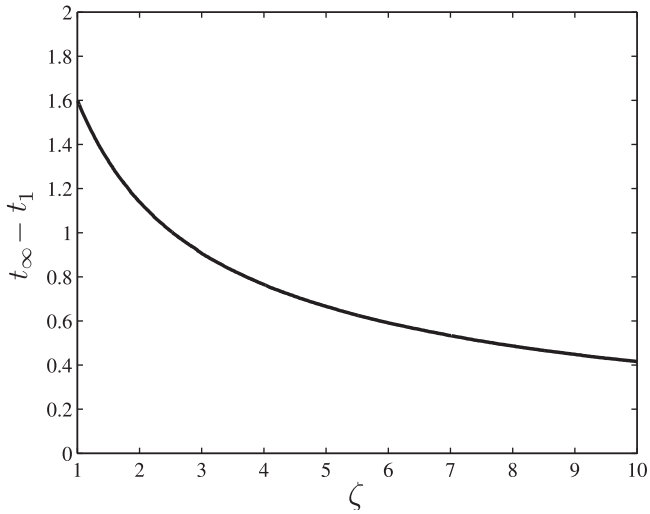

Figure 9. The time lapse $t_\infty - t_1$ for varying parameter ζ and $x_1(0) = -4$, $x_2(0) = -4$.

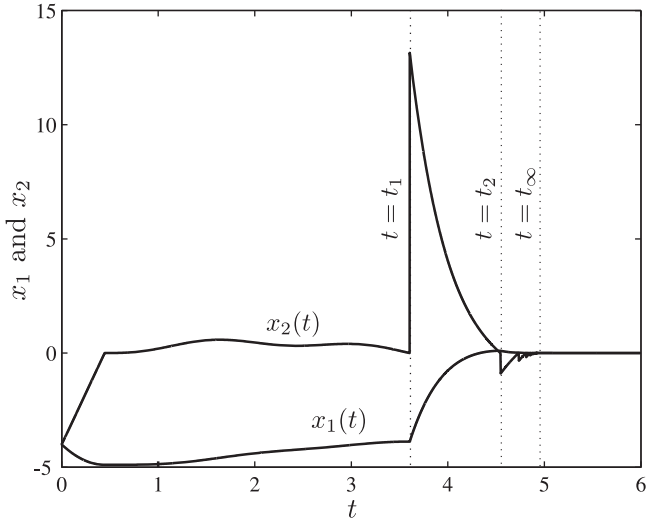

Figure 10. Time history of the position $x_1(t)$ and the velocity $x_2(t)$ for an uncertainty of 10% on the mass and $x_1(0) = -4$, $x_2(0) = -4$.

6. CONCLUSIONS

In this paper, we have provided a solution to the robust set-point stabilization problem for motion systems subject to uncertain friction. A robust stability guarantee with respect to frictional uncertainties is particularly relevant in practice, since uncertainties in the friction model are unavoidable. We propose an impulsive feedback control design, consisting of a non-impulsive state-feedback and a state-dependent impulsive feedback, that robustly stabilizes the set-point for a class of position-, velocity- and time-dependent friction laws with uncertainty. Moreover, this control strategy guarantees the finite-time convergence to the set-point, thereby inducing favorable transient performance characteristics in the resulting closed loop. The results are illustrated by means of a representative motion control example. Future work involves the extension of the current work in the direction of incorporating implementation issues such as the robustness in the face of measurement noise and the approximation of the force impulses.

DOI: 10.1002/rnc

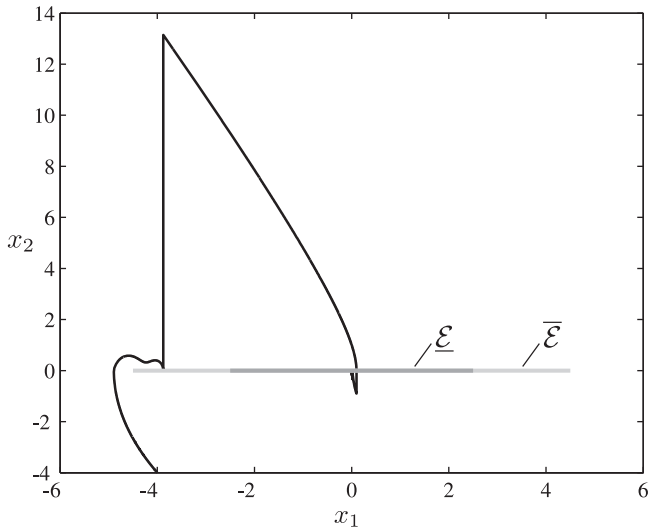

Figure 11. Phase portrait depicting $x_2(t)$ versus $x_1(t)$ for an uncertainty of 10% on the mass and $x_1(0)=-4$, $x_2(0)=-4$.

APPENDIX A: PROOFS

A.1. Proof of Proposition 1

By exploiting the Laplace transforms $X_i(s)=\mathscr{L}(x_i(t)), i=1,2$, $F(s)=\mathscr{L}(f(t))$, (15) can be transformed to $sX_1(s)-x_{10}=X_2(s)$, $sX_2(s)-x_{20}=-\omega_n^2X_1(s)-2\zeta\omega_nX_2(s)+F(s)$, and we obtain that it holds that $X_1(s)=S_1(s)x_{10}+S_2(s)x_{20}+S_2(s)F(s)$, where the $S_1(s)$ and $S_2(s)$ are the transfer functions of the initial conditions given by

$$S_1(s)=\frac{s+2\zeta\omega_n}{s^2+2\zeta\omega_ns+\omega_n^2}=\frac{\lambda_2}{\lambda_2-\lambda_1}\frac{1}{s-\lambda_1}-\frac{\lambda_1}{\lambda_2-\lambda_1}\frac{1}{s-\lambda_2}, \tag{A1}$$

$$S_2(s)=\frac{1}{s^2+2\zeta\omega_ns+\omega_n^2}=-\frac{1}{\lambda_2-\lambda_1}\frac{1}{s-\lambda_1}+\frac{1}{\lambda_2-\lambda_1}\frac{1}{s-\lambda_2}. \tag{A2}$$

We take the inverse Laplace transform of $S_1(s)$ and $S_2(s)$ to obtain the expressions for $s_1(t)$, $s_2(t)$ as in (21), for which it holds that $s_1(0)=1$, $s_2(0)=0$ and the following inequalities hold

$$\begin{aligned} &s_1(t)>0 \quad \forall t>-\frac{1}{\lambda_2-\lambda_1}\ln\left(\frac{\lambda_1}{\lambda_2}\right),\\ &s_2(t)>0 \quad \forall t>0. \end{aligned} \tag{A3}$$

Differentiation of (21) with respect to time gives

$$\begin{aligned} \dot{s}_1(t)&=-\lambda_1\lambda_2s_2(t),\\ \dot{s}_2(t)&=\frac{1}{\lambda_2-\lambda_1}(-\lambda_1e^{\lambda_1t}+\lambda_2e^{\lambda_2t})=s_1(t)+(\lambda_1+\lambda_2)s_2(t), \end{aligned} \tag{A4}$$

and it therefore holds that $\dot{s}_2(t)>0$ for $t<(1/(\lambda_2-\lambda_1))\ln(\lambda_1/\lambda_2)$ from which we conclude, using (A3), that

$$\dot{s}_2(t)>0 \quad \Longleftrightarrow \quad s_1(-t)>0. \tag{A5}$$

DOI: 10.1002/rnc

The general solution of (15), with the initial condition (17) and on a non-impulsive time-interval for which $x_2(t)\neq 0$ does not change sign, can therefore be written as

$$\begin{aligned} x_1(t) &= s_1(t-t_0)x_{10}+s_2(t-t_0)x_{20}+\int_{t_0}^{t} s_2(t-\tau)f(\tau)\,\mathrm{d}\tau,\\ x_2(t) &= \dot{s}_1(t-t_0)x_{10}+\dot{s}_2(t-t_0)x_{20}+\int_{t_0}^{t} \dot{s}_2(t-\tau)f(\tau)\,\mathrm{d}\tau. \end{aligned} \tag{A6}$$

We now decompose the input $f(t)$ in a constant input f_{const} and a time-varying input $f_{\text{var}}(t)$, i.e.

$$f(t)=\underbrace{-g\mu_{\text{const}}\,\text{sign}(x_2)}_{f_{\text{const}}}\underbrace{-g\left(\mu(t)-\mu_{\text{const}}\right)\text{sign}(x_2)}_{f_{\text{var}}(t)} \tag{A7}$$

for some $\mu_{\text{const}}>0$. The convolution integrals in (A6) of the constant input yield

$$\int_{t_0}^{t} s_2(t-\tau)f_{\text{const}}\,\mathrm{d}\tau=\left[\frac{f_{\text{const}}}{\lambda_1\lambda_2}s_1(t-\tau)\right]_{t_0}^{t}=\frac{f_{\text{const}}}{\lambda_1\lambda_2}(1-s_1(t-t_0)), \tag{A8}$$

$$\int_{t_0}^{t} \dot{s}_2(t-\tau)f_{\text{const}}\,\mathrm{d}\tau=[-f_{\text{const}}s_2(t-\tau)]_{t_0}^{t}=f_{\text{const}}s_2(t-t_0). \tag{A9}$$

If $x_2>0$ and $\mu_{\text{const}}=\underline{\mu}$, then it holds that $f_{\text{var}}(t)\leqslant 0$ for all t and, using the inequalities (A3), (A5), we arrive at the following inequalities for the convolution integrals of the time-varying input $f(\tau)$ in (A6):

$$\begin{aligned} &\int_{t_0}^{t} s_2(t-\tau)f_{\text{var}}(\tau)\,\mathrm{d}\tau\leqslant 0 \quad t-t_0\geqslant 0,\\ &\int_{t_0}^{t} \dot{s}_2(t-\tau)f_{\text{var}}(\tau)\,\mathrm{d}\tau\leqslant 0 \quad t-t_0\leqslant \frac{1}{\lambda_2-\lambda_1}\ln\frac{\lambda_1}{\lambda_2}. \end{aligned} \tag{A10}$$

Similarly, if $x_2>0$ and $\mu_{\text{const}}=\overline{\mu}$, then it holds that $f_{\text{var}}(t)\geqslant 0$ and the inequalities for the convolution integrals change sign. Let $(\underline{x}_1(t),\underline{x}_2(t))$ denote the solution of the initial value problem (15) and (17) for $\mu(t)=\underline{\mu}$ and $(\overline{x}_1(t),\overline{x}_2(t))$ for $\mu(t)=\overline{\mu}$. The latter two solutions for constant μ and positive velocity $x_2>0$ can be expressed in closed form as in (19) and (20). Similar expressions can obviously be derived for the case that $x_2<0$. The inequalities on the time-varying input in (A10) imply that, for a certain time-interval, the solution $(x_1(t),x_2(t))$ is lower and upper bounded by the solutions $(\underline{x}_1(t),\underline{x}_2(t))$ and $(\overline{x}_1(t),\overline{x}_2(t))$ according to (22).

A.2. Proof of Proposition 2

We first investigate the slope of $\mathsf{f}(t)$ given by

$$\mathsf{f}'(t)=\underline{c}\lambda_1\lambda_2 s_2(t_j-t)=-\underline{c}\frac{\lambda_1\lambda_2}{\lambda_2-\lambda_1}(\mathrm{e}^{\lambda_1(t_j-t)}-\mathrm{e}^{\lambda_2(t_j-t)}). \tag{A11}$$

It holds that $\mathsf{f}'(t_j)=0$ and $\mathsf{f}'(\underline{t}_{j+1})=-x_2^{+}(t_j)$. Further differentiation gives

$$\mathsf{f}''(t)=-\underline{c}\lambda_1\lambda_2\dot{s}_2(t_j-t)=-\underline{c}\frac{\lambda_1\lambda_2}{\lambda_2-\lambda_1}(-\lambda_1\mathrm{e}^{\lambda_1(t_j-t)}+\lambda_2\mathrm{e}^{\lambda_2(t_j-t)})=-\lambda_2\mathsf{f}'(t)-\underline{c}\lambda_1\lambda_2\mathrm{e}^{\lambda_1(t_j-t)}. \tag{A12}$$

The slope $\mathsf{f}'(t)$ is strictly negative on the open domain $t>t_j$. In addition, it can easily be checked that also $\mathsf{f}''(t)<-\underline{c}\omega_n^2<0$ on the domain $t>t_j$. We can therefore conclude that, for $\zeta>1$, the algebraic equation $\mathsf{f}(\underline{t}_{j+1})=0$ has a unique solution. Moreover, on the domain $t>t_j$, the function

DOI: 10.1002/rnc

f is bounded from above by a concave parabola, i.e. $\mathsf{f}(\underline{t}_{j+1}) < -\frac{1}{2}\underline{c}\omega_n^2(\underline{t}_{j+1}-t_j)^2 - x_1(t_j)$, and the end time therefore has the upper bound

$$\underline{t}_{j+1}-t_j < \sqrt{\frac{2|x_1(t_j)|}{\underline{c}\omega_n^2}} = \sqrt{\frac{2|x_1(t_j)|}{g\underline{\mu}}}. \tag{A13}$$

The value of $x_2^+(t_j)$ is determined by the evaluation of $\underline{x}_2(t)$, given by (25) at $t=t_j$ using the previously calculated value of $\underline{t}_{j+1}$. Since $\underline{t}_{j+1}$ is bounded, due to the fact that x_1 is bounded for all $(x_1, x_2)\in\overline{\mathscr{E}}$, also $x_2^+(t_j)$ is bounded.

Subsequently, the impulsive control action $k_3(x_1(t_j))$ can be computed from (28). Hence, $k_3(x_1)$ is uniquely defined and bounded for all $(x_1, x_2)\in\overline{\mathscr{E}}$ and the proof is complete.

A.3. Proof of Proposition 3

Consider the energy function $V(\boldsymbol{x})=\frac{1}{2}mx_2^2+\frac{1}{2}k_1x_1^2$. Define the set $\Omega=\{\boldsymbol{x}\in\mathbb{R}^2 \mid V(\boldsymbol{x}) > \frac{1}{2}k_1(mg\overline{\mu}/k_1)^2\}$. By definition of the impulsive part of the control law (9) no impulsive control action will occur for $\boldsymbol{x}\in\Omega$ because $\Omega\cap\overline{\mathscr{E}}=\emptyset$. Hence, using (11), the time-derivative of V along solutions of the closed-loop system can be evaluated with $\dot{V}=-k_2x_2^2-mg\mu(x_1,x_2,t)|x_2|\leqslant -k_2x_2^2-mg\underline{\mu}|x_2|$, for $\boldsymbol{x}\in\Omega$. The parameter $k_2(t)$ switches from $k_{21}>0$, for $t_0\leqslant t<t_1$, to a larger value $k_{22}>0$, for $t\geqslant t_1$. It holds that $\dot{V}\leqslant 0$ for $\boldsymbol{x}\in\Omega$, implying that solutions cannot grow unbounded along flows. The switching of k_2 such that $\zeta>1$ when the impulsive controller is switched on guarantees the satisfaction of the conditions of Proposition 2 and therewith implies that $U=k_3(x_1)$ is defined and bounded for all $\boldsymbol{x}\in\overline{\mathscr{E}}$, whereas $U=0$ for $\boldsymbol{x}\notin\overline{\mathscr{E}}$. The impulsive control force U is therefore bounded and leads to a bounded jump in x_2. Hence, the boundedness of solutions in forward time is guaranteed.

A.4. Proof of Proposition 6

Without loss of generality we study the case that $y_j:=\overline{x}_1(\overline{t}_j)<0$ and therefore $k_3(y_j)>0$. We study the system (11) with $\mu(t)=\overline{\mu}$ which obeys the following equation of motion

$$\begin{aligned}\dot{\overline{x}}_1(t) &= \overline{x}_2(t)\\ \dot{\overline{x}}_2(t) &= -\omega_n^2\overline{x}_1(t)-2\zeta\omega_n\overline{x}_2(t)-g\overline{\mu}\end{aligned} \tag{A14}$$

for $\overline{t}_j<t<\overline{t}_{j+1}$, where $\overline{t}_j$ are the impulse times corresponding to this system, and $\overline{x}_1(\overline{t}_j)<0$. Next we will derive the map $y_{j+1}=\overline{F}(y_j)$ with $y_j:=\overline{x}_1(\overline{t}_j)$. System (A14) has the closed form solution (20)

$$\begin{aligned}\overline{x}_1(t) &= s_1(t-\overline{t}_j)\overline{x}_1(\overline{t}_j)+s_2(t-\overline{t}_j)\overline{x}_2^+(\overline{t}_j)-\overline{c}(1-s_1(t-\overline{t}_j)),\\ \overline{x}_2(t) &= \dot{s}_1(t-\overline{t}_j)\overline{x}_1(\overline{t}_j)+\dot{s}_2(t-\overline{t}_j)\overline{x}_2^+(\overline{t}_j)-\lambda_1\lambda_2\overline{c}s_2(t-\overline{t}_j)\end{aligned} \tag{A15}$$

with the initial conditions $\overline{x}_1(\overline{t}_j)=y_j$, $\overline{x}_2^+(\overline{t}_j)=k_3(y_j)/m=:K_3(y_j)$. The time-lapse $\overline{t}_{j+1}-\overline{t}_j$ can be found from $\overline{x}_2(\overline{t}_{j+1})=\dot{s}_1(\overline{t}_{j+1}-\overline{t}_j)y_j+\dot{s}_2(\overline{t}_{j+1}-\overline{t}_j)K_3(y_j)-\lambda_1\lambda_2\overline{c}s_2(\overline{t}_{j+1}-\overline{t}_j)=0$. We substitute the functions $\dot{s}_1$, $\dot{s}_2$ and s_2, given in (21), (A4), and rearrange terms, which gives

$$\begin{aligned}&\left(\frac{\lambda_1\lambda_2}{\lambda_2-\lambda_1}(y_j+\overline{c})-\frac{\lambda_1}{\lambda_2-\lambda_1}K_3(y_j)\right)\mathrm{e}^{\lambda_1(\overline{t}_{j+1}-\overline{t}_j)}\\ &\quad+\left(-\frac{\lambda_1\lambda_2}{\lambda_2-\lambda_1}(y_j+\overline{c})+\frac{\lambda_2}{\lambda_2-\lambda_1}K_3(y_j)\right)\mathrm{e}^{\lambda_2(\overline{t}_{j+1}-\overline{t}_j)}=0.\end{aligned} \tag{A16}$$

The time-lapse $\overline{t}_{j+1}-\overline{t}_j$ is therefore given by

$$\overline{t}_{j+1}-\overline{t}_j=\frac{1}{\lambda_2-\lambda_1}\ln\left(\frac{y_j+\overline{c}-\frac{1}{\lambda_2}K_3(y_j)}{y_j+\overline{c}-\frac{1}{\lambda_1}K_3(y_j)}\right), \tag{A17}$$

DOI: 10.1002/rnc

which is bounded because $y_j \geqslant -\overline{c}$, i.e. $\overline{t}_{j+1}-\overline{t}_j \leqslant (1/(\lambda_2-\lambda_1))\ln(\lambda_1/\lambda_2)$. The return value y_{j+1} of the map equals $\overline{F}(y_j)=\overline{x}_1(\overline{t}_{j+1})$, which yields

$$\begin{aligned}\overline{F}(y_j) &= s_1(\overline{t}_{j+1}-\overline{t}_j)(y_j+\overline{c})+s_2(\overline{t}_{j+1}-\overline{t}_j)K_3(y_j)-\overline{c}\\ &= a_2\left(y_j+\overline{c}-\frac{K_3(y_j)}{\lambda_2}\right)\mathrm{e}^{\lambda_1(\overline{t}_{j+1}-\overline{t}_j)}+a_1\left(y_j+\overline{c}-\frac{K_3(y_j)}{\lambda_1}\right)\mathrm{e}^{\lambda_2(\overline{t}_{j+1}-\overline{t}_j)}-\overline{c}\end{aligned} \tag{A18}$$

with

$$a_1 := -\frac{\lambda_1}{\lambda_2-\lambda_1}, \quad a_2 := \frac{\lambda_2}{\lambda_2-\lambda_1}. \tag{A19}$$

Substitution of (A17) in (A18) gives

$$\begin{aligned}\overline{F}(y_j) = a_2&\left(y_j+\overline{c}-\frac{K_3(y_j)}{\lambda_2}\right)\left(\frac{y_j+\overline{c}-\frac{1}{\lambda_2}K_3(y_j)}{y_j+\overline{c}-\frac{1}{\lambda_1}K_3(y_j)}\right)^{-a_1}\\ &+a_1\left(y_j+\overline{c}-\frac{K_3(y_j)}{\lambda_1}\right)\left(\frac{y_j+\overline{c}-\frac{1}{\lambda_2}K_3(y_j)}{y_j+\overline{c}-\frac{1}{\lambda_1}K_3(y_j)}\right)^{a_2},\end{aligned} \tag{A20}$$

which can be simplified using $a_1+a_2=1$ to

$$\begin{aligned}\overline{F}(y_j) &= \left(\bar{c}+y_j-\frac{K_3(y_j)}{\lambda_2}\right)^{a_2}\left(\bar{c}+y_j-\frac{K_3(y_j)}{\lambda_1}\right)^{a_1}-\bar{c}\\ &= \bar{c}\left[\left(1+\frac{y_j}{\bar{c}}-\frac{K_3(y_j)}{\bar{c}\lambda_2}\right)^{a_2}\left(1+\frac{y_j}{\bar{c}}-\frac{K_3(y_j)}{\bar{c}\lambda_1}\right)^{a_1}-1\right].\end{aligned} \tag{A21}$$

Clearly, $\overline{F}(y)$ has a fixed point at $y^*=\overline{F}(y^*)$ if $K_3(y^*)=0$. The map $\overline{F}$ has therefore a unique fixed point at $y=0$.

In order to study the contraction properties of this map, we now would have to evaluate the derivative $\overline{F}'(y)$, but a direct evaluation of this derivative is obstructed by the fact that $K_3'(0)$ does not exist (note that $k_3'(0)$ does not exist due to (32) and (34)). Here, we use the Taylor expansion $(1+x)^a \approx 1+ax+(a(a-1)/2)x^2$ on each of the terms in the brackets in the expression (A21) and retain terms of $\mathcal{O}(y)$. Note that $K_3(y)=\mathcal{O}(\sqrt{y})$ and $K_3(y)^2=\mathcal{O}(y)$, see (35). For small values of y, we can therefore approximate $\overline{F}$ with

$$\begin{aligned}\overline{F}(y) = \bar{c}&\left[\left(1+a_2\frac{y}{\bar{c}}-a_2\frac{K_3(y)}{\lambda_2\bar{c}}+\frac{a_2(a_2-1)}{2}\frac{K_3^2(y)}{\lambda_2^2\bar{c}^2}\right)\right.\\ &\left.\cdot\left(1+a_1\frac{y}{\bar{c}}-a_1\frac{K_3(y)}{\lambda_1\bar{c}}+\frac{a_1(a_1-1)}{2}\frac{K_3^2(y)}{\lambda_1^2\bar{c}^2}\right)-1\right]+\mathcal{O}(y^{\frac{3}{2}})\\ = \bar{c}&\left[(a_1+a_2)\frac{y}{\bar{c}}-\left(\frac{a_2}{\lambda_2}+\frac{a_1}{\lambda_1}\right)\frac{K_3(y)}{\bar{c}}+\left(\frac{a_1a_2}{\lambda_1\lambda_2}+\frac{a_2(a_2-1)}{2\lambda_2^2}+\frac{a_1(a_1-1)}{2\lambda_1^2}\right)\frac{K_3^2(y)}{\bar{c}^2}\right]\\ &+\mathcal{O}(y^{\frac{3}{2}}).\end{aligned} \tag{A22}$$

The following coefficients appear in (A22): $a_1+a_2=1$, $(a_2/\lambda_2)+(a_1/\lambda_1)=0$, and

$$\frac{a_1a_2}{\lambda_1\lambda_2}+\frac{a_2(a_2-1)}{2\lambda_2^2}+\frac{a_1(a_1-1)}{2\lambda_1^2}=\frac{a_1a_2}{\lambda_1\lambda_2}-\frac{a_2a_1}{2\lambda_2^2}-\frac{a_1a_2}{2\lambda_1^2}=\frac{1}{2\lambda_1\lambda_2}=\frac{1}{2}\frac{1}{\omega_n^2}. \tag{A23}$$

DOI: 10.1002/rnc

Hence, the map $\overline{F}$ is approximated to leading order by

$$\overline{F}(y)=y+\frac{1}{2}\frac{1}{\omega_n^2}\frac{K_3^2(y)}{\bar{c}}+\mathcal{O}(y^{\frac{3}{2}}) \tag{A24}$$

and $k_3(y)\approx k_{3\text{approx}}(y)=-\operatorname{sign}(y)\sqrt{2\underline{c}\omega_n^2 m^2|y|}$ for small values of $|y|$, see (35). The slope of the map at the fixed point $y=0$, therefore, yields $\overline{F}'(0)=1-\underline{c}/\overline{c}=1-\underline{\mu}/\overline{\mu}$, which fulfills the condition $0\leqslant\overline{F}'(0)<1$ because $0<\underline{\mu}\leqslant\overline{\mu}$. Note that if another control law would have been chosen for which $K_3'(0)$ is bounded, then it would hold that $\overline{F}'(0)=1$. For $y\neq 0$, the slope $\overline{F}'(y)$ is much easier to obtain as $K_3'(y)$ is bounded for $y\neq 0$. For $y<0$ we have

$$\begin{aligned}\overline{F}'(y)=a_2&\left(1+\frac{y}{\bar{c}}-\frac{K_3(y)}{\bar{c}\lambda_2}\right)^{-a_1}\left(1+\frac{y}{\bar{c}}-\frac{K_3(y)}{\bar{c}\lambda_1}\right)^{a_1}\left(1-\frac{K_3'(y)}{\lambda_2}\right)\\&+a_1\left(1+\frac{y}{\bar{c}}-\frac{K_3(y)}{\bar{c}\lambda_1}\right)^{-a_2}\left(1+\frac{y}{\bar{c}}-\frac{K_3(y)}{\bar{c}\lambda_2}\right)^{a_2}\left(1-\frac{K_3'(y)}{\lambda_1}\right).\end{aligned} \tag{A25}$$

We introduce the following abbreviations:

$$\overline{L}_1=1+\frac{y}{\overline{c}}-\frac{K_3(y)}{\overline{c}\lambda_1},\quad \overline{L}_2=1+\frac{y}{\overline{c}}-\frac{K_3(y)}{\overline{c}\lambda_2},\quad Z_1=\left(1-\frac{K_3'(y)}{\lambda_1}\right), \tag{A26}$$

$$\underline{L}_1=1+\frac{y}{\underline{c}}-\frac{K_3(y)}{\underline{c}\lambda_1},\quad \underline{L}_2=1+\frac{y}{\underline{c}}-\frac{K_3(y)}{\underline{c}\lambda_2},\quad Z_2=\left(1-\frac{K_3'(y)}{\lambda_2}\right). \tag{A27}$$

Using these abbreviations, together with $a_1+a_2=1$, we write the slope $\overline{F}'(y)$ for $y<0$ as

$$\begin{aligned}\overline{F}'(y)&=a_2\overline{L}_2^{-a_1}\overline{L}_1^{a_1}Z_2+a_1\overline{L}_1^{-a_2}\overline{L}_2^{a_2}Z_1=a_2\left(\frac{\overline{L}_2}{\overline{L}_1}\right)^{a_2-1}Z_2+a_1\left(\frac{\overline{L}_2}{\overline{L}_1}\right)^{a_2}Z_1\\&=\left(\frac{\overline{L}_2}{\overline{L}_1}\right)^{a_2}\left(a_2\left(\frac{\overline{L}_1}{\overline{L}_2}\right)Z_2+a_1Z_1\right).\end{aligned} \tag{A28}$$

We now use the fact that $(a_2/\lambda_2)+(a_1/\lambda_1)=0$ and therefore $a_2Z_2+a_1Z_1=1$ to arrive at

$$\overline{F}'(y)=\left(\frac{\overline{L}_2}{\overline{L}_1}\right)^{a_2}\left(1+a_2Z_2\left(\frac{\overline{L}_1}{\overline{L}_2}-1\right)\right). \tag{A29}$$

It holds that $\underline{F}(y)=\underline{F}'(y)=0$ for $\mu(t)=\underline{\mu}$, so $0=1+a_2Z_2(\underline{L}_2/\underline{L}_1-1)$. Substitution of the latter gives

$$\overline{F}'(y)=\left(\frac{\overline{L}_2}{\overline{L}_1}\right)^{a_2}\left(1-\frac{\frac{\overline{L}_1}{\overline{L}_2}-1}{\frac{\underline{L}_1}{\underline{L}_2}-1}\right)=\left(\frac{\overline{L}_2}{\overline{L}_1}\right)^{a_2}\left(1-\frac{\overline{L}_1-\overline{L}_2}{\underline{L}_1-\underline{L}_2}\frac{\underline{L}_2}{\overline{L}_2}\right)=\left(\frac{\overline{L}_2}{\overline{L}_1}\right)^{a_2}\left(1-\frac{\underline{\mu}}{\overline{\mu}}\frac{\underline{L}_2}{\overline{L}_2}\right). \tag{A30}$$

Because $a_2>0$, $(\overline{L}_2/\overline{L}_1)<1$ and $(\underline{L}_2/\overline{L}_2)>1$ for $y<0$, it holds that the map $\overline{F}$ has its largest slope for $y=0$, i.e. $\overline{F}'(y)\leqslant 1-\underline{\mu}/\overline{\mu}$. The symmetry of the problem implies that $|\overline{F}(y)|\leqslant(1-\underline{\mu}/\overline{\mu})|y|$ for all y. The map $\overline{F}$ is therefore a contraction mapping, i.e.

$$|y_{j+1}|\leqslant\left(1-\frac{\underline{\mu}}{\overline{\mu}}\right)|y_j|, \tag{A31}$$

since $0\leqslant 1-(\underline{\mu}/\overline{\mu})<1$ due to the fact that $0<\underline{\mu}\leqslant\overline{\mu}$ by the adoption of Assumption 1. Hence, the sequence $y_j=\overline{x}_1(\overline{t}_j)$ converges to zero as $j\to\infty$.

DOI: 10.1002/rnc

A.5. Proof of Proposition 7

Without loss of generality, we consider the case $x_1(t_1)<0$. Let us first show that under Assumption 3 and (A31), it holds that $\overline{F}(-\overline{c})\geqslant(1-\underline{\mu}/\overline{\mu})\cdot(-\overline{c})>-\underline{c}$ for both cases in Assumption 3:

- If condition (39) in Assumption 3 holds (i.e. $\overline{\mu}<2\underline{\mu}$), then $|\overline{F}(-\overline{c})|<(\overline{c}/2)<\underline{c}$. $\overline{F}(y)$ is an even function with $\overline{F}(y)<0$ for $y<0$ which implies that $\overline{F}(-\overline{c})>-\underline{c}$;
- Note that (A21) implies that

$$\overline{F}(-\overline{c})=\left(-\frac{K_3(-\overline{c})}{\lambda_2}\right)^{a_2}\left(-\frac{K_3(-\overline{c})}{\lambda_1}\right)^{a_1}-\overline{c}=K_3(-\overline{c})(-\lambda_2)^{-1}\left(\frac{\lambda_2}{\lambda_1}\right)^{a_1}-\overline{c}, \tag{A32}$$

  where in the last equality we used that $a_1+a_2=1$. The inequality in (33) gives $K_3(y)>\lambda_2 y$ for $y<0$, which together with (A32) gives

$$\overline{F}(-\overline{c})>\overline{c}\left(\left(\frac{\lambda_2}{\lambda_1}\right)^{a_1}-1\right)=-\overline{c}\left(1-\left(\frac{\lambda_1}{\lambda_2}\right)^{-a_1}\right). \tag{A33}$$

  If condition (40) in Assumption 3 holds (i.e. $\underline{\mu}/\overline{\mu}>1-(\lambda_1/\lambda_2)^{-a_1}$), then (A33) gives $\overline{F}(-\overline{c})>-\overline{c}(\underline{\mu}/\overline{\mu})=-\underline{c}$.

Since $\overline{F}(-\overline{c})>-\underline{c}$, it holds that $x_1(t_2)>-\underline{c}$. Solutions can therefore only escape the set χ, see Figure 3, through the 'inner' part $-\underline{c}<x_1\leqslant 0$ of $\underline{\mathscr{E}}^-$. The stick set $\underline{\mathscr{E}}^-$ is, therefore, reached in a finite time, because the edges of the stick set $\mathscr{E}(t)\supseteq\underline{\mathscr{E}}$ cannot be reached (see [34, 35]). We can estimate the time lapse t_2-t_1 by evaluation of the condition $x_2^-(t_2)=0$ using the general solution as in (A6) with $t_0=t_2$ as reference time $x_2^+(t_1)=-\lambda_1\lambda_2 s_2(t_1-t_2)(x_1(t_2)+\underline{c})+\int_{t_2}^{t_1}\dot{s}_2(t_1-\tau)f_{\text{var}}(\tau)\,\mathrm{d}\tau$ with $f_{\text{var}}=-g(\mu(t)-\underline{\mu})\leqslant 0$. The inequalities $s_2(t)<0$, $\dot{s}_2(t)>1$ for $t<0$, together with $t_2>t_1$, give $x_2^+(t_1)>-\lambda_1\lambda_2 s_2(t_1-t_2)(x_1(t_2)+\underline{c})\geqslant-\lambda_1\lambda_2 s_2(t_1-t_2)(\overline{F}(-\overline{c})+\underline{c})$. Hence, we have that $K_3(x_1(t_1))>-\lambda_1\lambda_2 s_2(t_1-t_2)(\overline{F}(-\overline{c})+\underline{c})$, which, in turn, gives

$$s_2(t_1-t_2)>-\frac{K_3(x_1(t_1))}{\lambda_1\lambda_2(\overline{F}(-\overline{c})+\underline{c})}. \tag{A34}$$

Clearly, the time lapse t_2-t_1 satisfies

$$t_2-t_1<-s_2^{-1}\left(-\frac{K_3(x_1(t_1))}{\lambda_1\lambda_2(\overline{F}(-\overline{c})+\underline{c})}\right). \tag{A35}$$

Note that

- if condition (39) in Assumption 3 holds (i.e. $\overline{\mu}<2\underline{\mu}$), then $\overline{F}(-\overline{c})>-\overline{c}+\underline{c}\Rightarrow\overline{F}(-\overline{c})+\underline{c}>2\underline{c}-\overline{c}>0$;
- if condition (40) in Assumption 3 holds (i.e. $(\underline{\mu}/\overline{\mu})>1-(\lambda_1/\lambda_2)^{-a_1}$), then

$$\overline{F}(-\overline{c})>-\overline{c}\left(1-\left(\frac{\lambda_1}{\lambda_2}\right)^{-a_1}\right), \tag{A36}$$

  which implies that

$$\overline{F}(-\overline{c})+\underline{c}>\underline{c}-\overline{c}\left(1-\left(\frac{\lambda_1}{\lambda_2}\right)^{-a_1}\right)=\frac{g}{\lambda_1\lambda_2}\left(\underline{\mu}-\overline{\mu}\left(1-\left(\frac{\lambda_1}{\lambda_2}\right)^{-a_1}\right)\right)>0. \tag{A37}$$

Consequently, the upper bound in (A35) on the time lapse t_2-t_1 is finite. The function $s_2(t)$ is strictly increasing for $t<0$ as $\dot{s}_2(t)>1$ and it therefore holds that $s_2(t)<t$ for $t<0$, and

DOI: 10.1002/rnc

correspondingly $s_2^{-1}(x)>x$ for $x<0$. The time lapse t_2-t_1 can, therefore, be bounded from above as follows:

- if condition (39) in Assumption 3 holds (i.e. $\overline{\mu}<2\underline{\mu}$):

$$t_2-t_1<\frac{K_3(x_1(t_1))}{(2\underline{c}-\overline{c})\lambda_1\lambda_2}=\frac{K_3(x_1(t_1))}{g(2\underline{\mu}-\overline{\mu})}; \tag{A38}$$

- if condition (40) in Assumption 3 holds (i.e. $(\underline{\mu}/\overline{\mu})>1-(\lambda_1/\lambda_2)^{-a_1}$):

$$t_2-t_1<\frac{K_3(x_1(t_1))}{g\left(\underline{\mu}-\overline{\mu}\left(1-\left(\frac{\lambda_1}{\lambda_2}\right)^{-a_1}\right)\right)}. \tag{A39}$$

A.6. Proof of Proposition 8

Using (25) for $t=t_j$, $\underline{x}_1(t_j)=-\underline{c}(1-s_1(t_j-\underline{t}_{j+1}))$ and the inequality $-\underline{c}\leqslant\underline{x}_1(t_j)$, because $\boldsymbol{x}^-(t_j)\in\underline{\mathscr{E}}^-$, we find that $s_1(t_j-\underline{t}_{j+1})\geqslant 0$ and, using (A3), it therefore holds that $\underline{t}_{j+1}-t_j\leqslant(1/(\lambda_2-\lambda_1))\ln(\lambda_1/\lambda_2)$. Hence, (22) in Proposition 1 holds, implying that the solution $\boldsymbol{x}(t)$ is wedged between $\underline{\boldsymbol{x}}(t)$ and $\overline{\boldsymbol{x}}(t)$, i.e. $\overline{x}_1(t)\leqslant x_1(t)\leqslant\underline{x}_1(t)$, $\overline{x}_2(t)\leqslant x_2(t)\leqslant\underline{x}_2(t)$, for those $t\in(t_j,\underline{t}_{j+1})$ such that the velocities $\overline{x}_2(t)$, $x_2(t)$ and $\underline{x}_2(t)$ are strictly positive. We, therefore, deduce that $\overline{t}_{j+1}\leqslant t_{j+1}\leqslant\underline{t}_{j+1}$. The time-instant $\overline{t}_{j+1}$ is a lower bound for t_{j+1} and can be found from $\overline{x}_2(\overline{t}_{j+1})=0$. By using the general solution (20) and taking $t_0=t_j$ as reference-time we obtain the expression

$$\overline{x}_2(\overline{t}_{j+1})=\dot{s}_1(\overline{t}_{j+1}-t_j)x_1(t_j)+\dot{s}_2(\overline{t}_{j+1}-t_j)x_2^+(t_j)-\lambda_1\lambda_2\overline{c}s_2(\overline{t}_{j+1}-t_j)=0. \tag{A40}$$

We substitute the functions $\dot{s}_1$, $\dot{s}_2$ and s_2 and rearrange terms, which gives

$$\left(\frac{\lambda_1\lambda_2}{\lambda_2-\lambda_1}(x_1(t_j)+\overline{c})-\frac{\lambda_1}{\lambda_2-\lambda_1}x_2^+(t_j)\right)\mathrm{e}^{\lambda_1(\overline{t}_{j+1}-t_j)} + \left(-\frac{\lambda_1\lambda_2}{\lambda_2-\lambda_1}(x_1(t_j)+\overline{c})+\frac{\lambda_2}{\lambda_2-\lambda_1}x_2^+(t_j)\right)\mathrm{e}^{\lambda_2(\overline{t}_{j+1}-t_j)}=0. \tag{A41}$$

Further rearranging terms and taking the natural logarithm yields the time-lapse

$$\overline{t}_{j+1}-t_j=\frac{1}{\lambda_2-\lambda_1}\ln\left(\frac{-\lambda_1\lambda_2(x_1(t_j)+\overline{c})+\lambda_1x_2^+(t_j)}{-\lambda_1\lambda_2(x_1(t_j)+\overline{c})+\lambda_2x_2^+(t_j)}\right), \tag{A42}$$

which is strictly positive for $x_2^+(t_j)>0$, because $-\underline{c}\leqslant x_1(t_j)\leqslant 0$. Similarly, we obtain the time-lapse

$$\underline{t}_{j+1}-t_j=\frac{1}{\lambda_2-\lambda_1}\ln\left(\frac{-\lambda_1\lambda_2(x_1(t_j)+\underline{c})+\lambda_1x_2^+(t_j)}{-\lambda_1\lambda_2(x_1(t_j)+\underline{c})+\lambda_2x_2^+(t_j)}\right), \tag{A43}$$

which gives the upper bound $\underline{t}_{j+1}$ for t_{j+1}. Clearly, the upper bound (A13) for $\underline{t}_{j+1}$ is also an alternative upper bound for t_{j+1}.

A.7. Proof of Proposition 10

The time difference between two consecutive impacts is bounded from above by (A13) with $x_1(t_j)=y_j$, i.e. $t_{j+1}-t_j\leqslant\sqrt{2|y_j|/(\underline{c}\omega_n^2)}=\sqrt{2|y_j|/(g\underline{\mu})}$. The total time to arrive at the origin amounts to

$$T:=t_\infty-t_2=\sum_{j=2}^{\infty}t_{j+1}-t_j\leqslant\sqrt{\frac{2}{g\underline{\mu}}}\sum_{j=2}^{\infty}\sqrt{|y_j|}. \tag{A44}$$

DOI: 10.1002/rnc

Recursive usage of the contraction property in (A31) yields

$$|y_j| \leqslant \left(1-\frac{\underline{\mu}}{\bar{\mu}}\right)^{j-2} |y_2|. \tag{A45}$$

Inequality (A45) in combination with (A44) gives the upper bound

$$T \leqslant \sqrt{\frac{2|y_2|}{g\underline{\mu}}} \sum_{j=2}^{\infty} \left(1-\frac{\underline{\mu}}{\bar{\mu}}\right)^{\frac{1}{2}j-1} = \sqrt{\frac{2|y_2|}{g\underline{\mu}}} \sum_{j=0}^{\infty} \left(1-\frac{\underline{\mu}}{\bar{\mu}}\right)^{\frac{1}{2}j}. \tag{A46}$$

Using the convergent geometric series

$$\sum_{j=0}^{\infty} x^{1/2j} = \sum_{j=0}^{\infty} (x^{1/2})^j = 1/(1-x^{1/2}) \quad |x|<1, \tag{A47}$$

we can give the conservative estimate

$$T \leqslant \sqrt{\frac{2|y_2|}{g\underline{\mu}}} \sum_{j=0}^{\infty} \left(1-\frac{\underline{\mu}}{\bar{\mu}}\right)^{\frac{1}{2}j} = \sqrt{\frac{2|y_2|}{g\underline{\mu}}} \frac{1}{1-\left(1-\frac{\underline{\mu}}{\bar{\mu}}\right)^{\frac{1}{2}}}, \tag{A48}$$

which gives an upper bound for the finite attraction time. Since $|y_2| \leqslant \underline{c}$ is bounded and Assumption 1 is satisfied, we can conclude that the attraction is symptotic.

A.8. Proof of Theorem 1

Consider the candidate Lyapunov function $V(\boldsymbol{x}) = \frac{1}{2}mx_2^2 + \frac{1}{2}k_1x_1^2$ and with some abuse of notation $V(t) = V(\boldsymbol{x}^+(t))$, i.e. the function $V(t)$ is right-continuous. Let us denote the value of the Lyapunov function $V(t_j)$ at impulse time-instants t_j by $V_j := V(t_j) = \frac{1}{2}m(x_2^+(t_j))^2 + \frac{1}{2}k_1x_1^2(t_j)$. Using the notation $y_j = x_1(t_j)$ and the fact that $x_2^+(t_j) = k_3(x_1(t_j))/m = K_3(y_j)$, the increment $V_{j+1} - V_j$ satisfies:

$$V_{j+1} - V_j = \tfrac{1}{2}k_1(y_{j+1}^2 - y_j^2) + \tfrac{1}{2}m(K_3^2(y_{j+1}) - K_3^2(y_j)). \tag{A49}$$

Propositions 6, 7 and 9 prove the contraction properties (A31): $|y_{j+1}| \leqslant (1-\underline{\mu}/\overline{\mu})|y_j|$, for $j \geqslant 1$. Moreover, the impulsive control law $K_3(y)$ is monotonically decreasing, see e.g. (31) in Section 3.2.1, i.e. $(K_3(y_2) - K_3(y_1))(y_2 - y_1) < 0 \ \forall y_1, y_2$. It therefore holds that $|K_3(y_{j+1})| < |K_3(y_j)|$ as well as

$$K_3^2(y_{j+1}) - K_3^2(y_j) < 0. \tag{A50}$$

Using (A50) and Assumption 1 in (A49) yields

$$V_{j+1} - V_j < \frac{1}{2}k_1(y_{j+1}^2 - y_j^2) < \frac{1}{2}k_1 \left(\left(1-\frac{\underline{\mu}}{\bar{\mu}}\right)^2 - 1\right) y_j^2 < 0 \tag{A51}$$

for $y_j \neq 0$. In other words, the Lyapunov function strictly decreases along the impulse time instants t_j. Let us now investigate the evolution of the Lyapunov function in between the impulse times (i.e. for $t \in (t_j, t_{j+1})$): $\dot{V} = -k_2x_2^2 - mg\mu(x_1, x_2, t)|x_2| \leqslant -k_2x_2^2 - mg\underline{\mu}|x_2|$. Since $x_2(t) \neq 0$ for all

DOI: 10.1002/rnc

$t\in(t_j,t_{j+1})$ we have that $V(t)<V_j$, for $t\in(t_j,t_{j+1})$, $j\geqslant 1$. Moreover, it holds that $\dot{V}(t)\leqslant 0$ for $t\in[t_0,t_1)$. Let us define $\overline{V}_0:=\max(V_0,V_1)$. We can construct a function $\beta_V(\overline{V}_0,t)$ as follows:

$$\beta_V(\overline{V}_0,t-t_0)=\begin{cases}\overline{V}_0 & t_0\leqslant t<t_2\\ \dfrac{V_2-\overline{V}_0}{t_3-t_2}(t-t_2)+\overline{V}_0 & t_2\leqslant t<t_3\\ \dfrac{V_j-V_{j-1}}{t_{j+1}-t_j}(t-t_j)+V_{j-1} & t_j\leqslant t<t_{j+1},\ j>2\\ 0 & t\geqslant t_\infty,\end{cases} \tag{A52}$$

such that

$$V(t)\leqslant\beta_V(\overline{V}_0,t-t_0),\quad t\geqslant t_0, \tag{A53}$$

where we used that $V(t_\infty)=0$ because $\boldsymbol{x}(t_\infty)=\boldsymbol{0}$, see Proposition 10. Clearly, $\beta_V(\overline{V}_0,t-t_0)$ is a continuous function of $\overline{V}_0$ and a continuous function of t because $\lim_{j\to\infty}V_j=0$. For fixed $t-t_0$, the mapping $\beta_V(\overline{V}_0,t-t_0)$ is upper bounded by a class $\mathscr{K}_\infty$ function with respect to $\overline{V}_0$. Moreover, since V_j, $j\geqslant 1$, is a strictly decreasing series tending to zero, see (A51), we have that, for fixed $\overline{V}_0$, the mapping $\beta_V(\overline{V}_0,t-t_0)$ is decreasing with respect to $t-t_0$ and $\beta_V(\overline{V}_0,t-t_0)=0$ for $t\geqslant t_\infty$ (where t_∞ is bounded, see Proposition 11). Hence, β_V is upper bounded by a class $\mathscr{KL}$ function $\overline{\beta}_V(\overline{V}_0,t-t_0):=\beta_V(\overline{V}_0,t-t_0)+\varepsilon\overline{V}_0\mathrm{e}^{(t_0-t)}$, with $\varepsilon>0$. Hence, we can conclude that $V(t)$ is upper bounded by a class $\mathscr{KL}$ function according to

$$V(t)\leqslant\overline{\beta}_V(\overline{V}_0,t-t_0),\quad t\geqslant t_0. \tag{A54}$$

Since it holds that $\alpha_1(|\boldsymbol{x}|)\leqslant V(\boldsymbol{x})\leqslant\alpha_2(|\boldsymbol{x}|)$, with $\alpha_1(|\boldsymbol{x}|):=\min(k_1/2,m/2)|\boldsymbol{x}|^2$ and $\alpha_2(|\boldsymbol{x}|):=\max(k_1/2,m/2)|\boldsymbol{x}|^2$, we can conclude from (A54) that

$$|\boldsymbol{x}(t)|\leqslant\alpha_1^{-1}\circ\overline{\beta}_V(\overline{V}_0,t-t_0),\quad t\geqslant t_0. \tag{A55}$$

Next, let us use that $\overline{V}_0=\max(V_0,V_1)\leqslant\max(\alpha_2(|\boldsymbol{x}(t_0)|),\alpha_2(|\boldsymbol{x}^+(t_1)|))=\alpha_2(\max(|\boldsymbol{x}(t_0)|,|\boldsymbol{x}^+(t_1)|))$, since $\alpha_2(\cdot)$ is a $\mathscr{K}_\infty$-function. Combining the latter fact with (A55) yields

$$|\boldsymbol{x}(t)|\leqslant\alpha_1^{-1}\circ\overline{\beta}_V(\alpha_2(\max(|\boldsymbol{x}(t_0)|,|\boldsymbol{x}^+(t_1)|)),t-t_0),\quad t\geqslant t_0. \tag{A56}$$

Consider a class $\mathscr{K}_\infty$-function $\gamma(\cdot)$ such that $\gamma(|\boldsymbol{x}^-(t_1)|)\geqslant(x_1^-(t_1))^2+K_3^2(x_1^-(t_1))\ \forall x^-(t_1)\in\overline{\mathscr{E}}$, which indeed exists and only depends on $|\boldsymbol{x}^-(t_1)|$ because of the symmetry properties and boundedness of K_3 and the fact that $|\boldsymbol{x}^-(t_1)|=|x_1^-(t_1)|$. Consequently, $|\boldsymbol{x}^+(t_1)|=(x_1^-(t_1))^2+K_3^2(x_1^-(t_1))\leqslant\gamma(|\boldsymbol{x}^-(t_1)|)$ and in turn it holds that $V(\boldsymbol{x}^+(t_1))\leqslant\alpha_2(\gamma(|\boldsymbol{x}^-(t_1)|))$. Combining the latter fact with the implication $V(\boldsymbol{x}^-(t_1))\leqslant V(\boldsymbol{x}(t_0))\Rightarrow\alpha_1^{-1}\circ\alpha_2(|\boldsymbol{x}(t_0)|)\geqslant|\boldsymbol{x}^-(t_1)|$ gives $V(\boldsymbol{x}^+(t_1))\leqslant\alpha_2\circ\gamma\circ\alpha_1^{-1}\circ\alpha_2(|\boldsymbol{x}(t_0)|)$. Consequently, we can conclude that $|\boldsymbol{x}^+(t_1)|\leqslant\alpha_1^{-1}\circ\alpha_2\circ\gamma\circ\alpha_1^{-1}\circ\alpha_2(|\boldsymbol{x}(t_0)|)$. Combining the latter fact with (A56) yields

$$|\boldsymbol{x}(t)|\leqslant\alpha_1^{-1}\circ\overline{\beta}_V(\alpha_2(\max(|\boldsymbol{x}(t_0)|,\alpha_1^{-1}\circ\alpha_2\circ\gamma\circ\alpha_1^{-1}\circ\alpha_2(|\boldsymbol{x}(t_0)|))),t-t_0),\quad t\geqslant t_0. \tag{A57}$$

If we define $\overline{\alpha}_2(|\boldsymbol{x}(t_0)|):=\alpha_2(\max(|\boldsymbol{x}(t_0)|,\alpha_1^{-1}\circ\alpha_2\circ\gamma\circ\alpha_1^{-1}\circ\alpha_2(|\boldsymbol{x}(t_0)|)))$, this inequality can be written as

$$|\boldsymbol{x}(t)|\leqslant\alpha_1^{-1}\circ\overline{\beta}_V(\overline{\alpha}_2(|\boldsymbol{x}(t_0)|),t-t_0)=:\beta_x(|\boldsymbol{x}(t_0)|,t-t_0),\quad t\geqslant t_0, \tag{A58}$$

where $\beta_x(s,t)$ is a class $\mathscr{KL}$ function, since $\overline{\alpha}_2$ is a class $\mathscr{K}_\infty$-function and $\overline{\beta}_V(s,t)$ is a class $\mathscr{KL}$ function. In other words the equilibrium point is globally uniformly asymptotically stable. Moreover, since all solutions of the system converge to the origin in finite time, see Proposition 11, the origin is globally uniformly symptotically stable. This completes the proof.

DOI: 10.1002/rnc

ACKNOWLEDGEMENTS

This work is partially supported by the Netherlands Organization for Scientific Research (NWO).

REFERENCES

1. Armstrong-Hélouvry B. *Control of Machines with Friction*. Kluwer Academic Publishers: Boston, 1991.
2. Canudas de Wit C. Robust control for servo-mechanisms under inexact friction compensation. *Automatica* 1993; **29**(3):757–761.
3. Armstrong-Hélouvry B, Dupont P, Canudas de Wit C. A survey of models, analysis tools and compensation methods for the control of machines with friction. *Automatica* 1994; **30**(7):1083–1138.
4. Canudas de Wit C, Olsson H, Åström K, Lischinsky P. A new model for control of systems with friction. *IEEE Transactions on Automatic Control* 1995; **40**(3):419–425.
5. Olsson H, Åström KJ, Canudas de Wit C, Gäfvert M, Lischinsky P. Friction models and friction compensation. *European Journal of Control* 1998; **4**(3):176–195.
6. Hensen RHA, Van de Molengraft MJG, Steinbuch M. Friction induced hunting limit cycles: a comparison between the LuGre and switch friction model. *Automatica* 2003; **39**:2131–2137.
7. Mallon NJ, van de Wouw N, Putra D, Nijmeijer H. Friction compensation in a controlled one-link robot using a reduced-order observer. *IEEE Transactions on Control Systems Technology* 2006; **14**(2):374–383.
8. Putra D, van de Wouw N, Nijmeijer H. Analysis of undercompensation and overcompensation of friction in 1DOF mechanical systems. *Automatica* 2007; **43**(8):1387–1394.
9. Southward S, Radcliffe C, MacCluer C. Robust nonlinear stick-slip friction compensation. *ASME Journal of Dynamic Systems*, *Measurement*, *and Control* 1991; **113**:639–644.
10. Johnson C, Lorenz R. Experimental identification of friction and its compensation in precise position controlled mechanisms. *IEEE Transactions on Industry Applications* 1992; **28**(6):1392–1398.
11. Altpeter F. Friction modeling, identification and compensation. *Ph.D. thesis*, Dept. Genie Mech., Ecole Polytech. Fed. Lausanne, Switzerland, 1999.
12. Papadopoulos EG, Chasparis GC. Analysis and model-based control of servomechanisms with friction. *Proceedings of the 2002 IEEE/RSJ International Conference on Intelligent Robots and Systems*, Lausanne, Switzerland, 2002; 2109–2114.
13. Panteley E, Ortega R, Gäfvert M. An adaptive friction compensator for global tracking in robot manipulators. *Systems and Control Letters* 1998; **33**:307–313.
14. Taware A, Tao G, Pradhan N, Teolis C. Friction compensation for a sandwich dynamic system. *Automatica* 2003; **39**(3):481–488.
15. Ipri S, Asada H. Tuned dither for friction suppression during force-guided robotic assembly. *Proceedings of the 1995 IEEE/RSJ International Conference on Intelligent Robots and Systems*, Pittsburgh, PA, U.S.A., vol. 1, 1995; 310–315.
16. Iannelli L, Johansson KH, Jönsson UT, Vasca F. Averaging of nonsmooth systems using dither. *Automatica* 2006; **42**:669–676.
17. Thomsen JJ. Using fast vibrations to quench friction-induced oscillations. *Journal of Sound and Vibration* 1999; **228**(5):1079–1102.
18. Yang S, Tomizuka M. Adaptive pulse width control for precise positioning under the influence of stiction and Coulomb friction. *ASME Journal of Dynamic Systems*, *Measurement and Control* 1988; **110**(3):221–227.
19. Hojjat Y, Higuchi T. Application of electromagnetic impulsive force to precise positioning. *International Journal of the Japan Society for Precision Engineering* 1991; **25**(11):39–44.
20. Yamagata Y, Higuchi T. A micropositioning device for precision automatic assembly using impact force of piezoelectric elements. *Proceedings of the IEEE International Conference on Robotics and Automation*, Nagoya, Aichi, Japan, 1995; 666–671.
21. Hägglund T. A friction compensator for pneumatic control valves. *Journal of Process Control* 2002; **12**:897–904.
22. Huang W. Impulsive manipulation. *Ph.D. Thesis*, Carnegie Mellon University, U.S.A. 1997.
23. Huang W, Mason W. Mechanics, planning, and control for tapping. *The International Journal of Robotics Research* 2000; **19**(10):883–894.
24. Kased R, Singh T. High precision point-to-point maneuvering of an experimental structure subject to friction via adaptive impulsive control. *Proceedings of the 2006 IEEE International Conference on Control Applications*, Germany, 2006; 3235–3240.
25. Kim J, Singh T. Desensitized control of vibratory systems with friction: linear programming approach. *Optimal Control Applications and Methods* 2004; **25**:165–180.
26. Siebenhaar C. Precise adjustment method using stroke impulse and friction. *Precision Engineering* 2004; **28**:194–203.
27. Wu R, Tung P. Fast pointing control for systems with stick-slip friction. *ASME Journal of Dynamic Systems*, *Measurement and Control* 2004; **126**:614–626.
28. Orlov Y, Santiesteban R, Aguilar LT. Impulsive control of a mechanical oscillator with friction. *Proceedings of the 2009 IEEE American Control Conference*, St. Louis, U.S.A., 2009; 3494–3499.
29. van de Wouw N, Leine RI. Robust impulsive control of motion systems with uncertain friction. *Technical Report DC2010.031*, Eindhoven University of Technology, Eindhoven, The Netherlands, 2010.

DOI: 10.1002/rnc

30. Moreau JJ. Unilateral contact and dry friction in finite freedom dynamics. In *Non-Smooth Mechanics and Applications*. Moreau JJ, Panagiotopoulos PD (eds). CISM Courses and Lectures, vol. 302. Springer: Wien, 1988; 1–82.
31. Acary V, Brogliato B. *Numerical Methods for Nonsmooth Dynamical Systems. Applications in Mechanics and Electronics*. Lecture Notes in Applied and Computational Mechanics, vol. 35. Springer: Berlin, Heidelberg, 2008.
32. Leine RI, van de Wouw N. *Stability and Convergence of Mechanical Systems with Unilateral Constraints*. Lecture Notes in Applied and Computational Mechanics, vol. 36. Springer: Berlin, 2008.
33. Glocker Ch. *Set-Valued Force Laws*, *Dynamics of Non-Smooth Systems*. Lecture Notes in Applied Mechanics, vol. 1. Springer: Berlin, 2001.
34. Díaz JI, Millot V. Coulomb friction and oscillation: stabilization in finite time for a system of damped oscillators. *XVIII CEDYA*: *Congress on Differential Equations and Applications/VIII CMA*: *Congress on Applied Mathematics*, Tarragona, 2003.
35. Cabot A. Stabilization of oscillators subject to dry friction: finite time convergence versus exponential decay results. *Transactions of the American Mathematical Society* 2008; **360**(1):103–121.
36. Leine RI, Nijmeijer H. *Dynamics and Bifurcations of Non-Smooth Mechanical Systems*. Lecture Notes in Applied and Computational Mechanics, vol. 18. Springer: Berlin, 2004.

DOI: 10.1002/rnc